

NASA TECHNICAL NOTE



NASA TN D-6850

2.1

NASA TN D-6850

LOAN COPY: RETURN
AFWL (DOUL)
KIRTLAND AFB, N.



APOLLO EXPERIENCE REPORT -
LUNAR MODULE LANDING GEAR SUBSYSTEM

by William F. Rogers
Manned Spacecraft Center
Houston, Texas 77058





0133650

1. Report No. NASA TN D-6850	2. Government Accession No.	3. Recipient's Catalog No.	
4. Title and Subtitle APOLLO EXPERIENCE REPORT LUNAR MODULE LANDING GEAR SUBSYSTEM		5. Report Date June 1972	
		6. Performing Organization Code	
7. Author(s) William F. Rogers, MSC		8. Performing Organization Report No. MSC S-316	
		10. Work Unit No. 914-13-20-13-72.	
9. Performing Organization Name and Address Manned Spacecraft Center Houston, Texas 77058		11. Contract or Grant No.	
		13. Type of Report and Period Covered Technical Note	
12. Sponsoring Agency Name and Address National Aeronautics and Space Administration Washington, D.C. 20546		14. Sponsoring Agency Code	
		Supplementary Notes The MSC Director waived the use of the International System of Units (SI) for this Apollo Experience Report, because, in his judgment, use of SI Units would impair the usefulness of the report or result in excessive cost.	
16. Abstract The development of the lunar module landing gear subsystem through the Apollo 11 lunar-landing mission is presented. The landing-gear design evolved from the design requirements, which had to satisfy the structural, mechanical, and landing-performance constraints of the vehicle. Extensive analyses and tests were undertaken to verify the design adequacy. Techniques of the landing-performance analysis served as a primary tool in developing the subsystem hardware and in determining the adequacy of the landing gear for toppling stability and energy absorption. The successful Apollo 11 lunar-landing mission provided the first opportunity for a complete flight test of the landing gear under both natural and induced environments.			
17. Key Words (Suggested by Author(s))		18. Distribution Statement	
<ul style="list-style-type: none"> * Landing Gear * Lunar Module * Landing Dynamics * Landing Performance * Landing-Gear Testing 		<ul style="list-style-type: none"> * Spacecraft Mechanisms * Lunar Landing 	
19. Security Classif. (of this report) None	20. Security Classif. (of this page) None	21. No. of Pages 58	22. Price* \$3.00



CONTENTS

Section	Page
SUMMARY	1
INTRODUCTION	1
DESIGN REQUIREMENTS AND CRITERIA	2
DEVELOPMENT HISTORY	4
CONFIGURATION DESCRIPTION	6
MAJOR PROBLEMS	9
Redesign of the 167-Inch-Tread-Radius Landing Gear	9
Statistical Landing Performance	10
Thermal Insulation	12
Weight Summary	13
Failure History	14
APOLLO 11 FLIGHT-TEST RESULTS	16
CONCLUDING REMARKS	20
REFERENCES	21
APPENDIX A — LANDING PERFORMANCE OF THE LM	22
APPENDIX B — HARDWARE DEVELOPMENT AND CERTIFICATION TESTING	33
APPENDIX C — DETAILED CONFIGURATION DESCRIPTION	46

TABLES

Table		Page
I	SIGNIFICANT LANDING-GEAR DESIGN CONCEPTS	5
II	LANDING-GEAR THERMAL-INSULATION WEIGHT HISTORY	12
III	APOLLO 11 LANDING-GEAR-COMPONENT WEIGHT SUMMARY	14
IV	LANDING-GEAR FAILURE HISTORY	15
V	APOLLO 11 (LM-5) STRUT-STROKE ESTIMATES	19
A-I	LANDING-PERFORMANCE HISTORY OF THE LM	31
B-I	LANDING-GEAR DEPLOYMENT-TEST SUMMARY	35
B-II	LANDING-GEAR DROP-TEST SUMMARY	36
B-III	CERTIFICATION SUMMARY OF THE LM LANDING-GEAR SUBSYSTEM	41
B-IV	COMPARISON OF CERTIFIED AND FLIGHT-CONFIGURATION HARDWARE	42

FIGURES

Figure	Page
1 The LM configuration (contractor technical proposal)	3
2 Stowed and deployed positions of the landing gear	5
3 The LM supported in the SLA	7
4 The LM landing gear	7
5 Overall view of the LM with the landing gear deployed	8
6 Landing-gear primary strut	8
7 Primary-strut compression load as a function of compression stroke	8
8 Landing-gear secondary strut	8
9 Secondary-strut compression and tension loads	
(a) Compression load as a function of compression stroke	9
(b) Tension load as a function of tension stroke	9
10 Final-landing-gear landing performance	10
11 Critical landing conditions	10
12 Apollo 11 attitude and motion touchdown conditions	11
13 The LM weight history	
(a) The LM touchdown weight history	13
(b) The LM landing-gear weight history	14
14 Apollo 11 LM (LM-5) on the lunar surface	16
15 Apollo 11 LM (LM-5) minus -Z (aft) footpad	16
16 Apollo 11 (LM-5) attitudes and attitude rates at touchdown	
(a) Pitch angle as a function of time	17
(b) Roll angle as a function of time	17
(c) Yaw angle as a function of time	17
(d) Pitch rate as a function of time	17
(e) Roll rate as a function of time	18
(f) Yaw rate as a function of time	18

Figure	Page
17 Apollo 11 (LM-5) descent-engine skirt	20
A-1 Validation of touchdown-analysis mathematical model	22
A-2 Lunar-surface description	
(a) Slope profile	25
(b) Protuberance profile	25
A-3 One-sixth-scale drop-test model	26
A-4 One-sixth-scale model and drop-test equipment at the prime contractor facility	27
A-5 One-sixth-scale-model test/analysis gross correlation for symmetrical drops	27
A-6 One-sixth-scale-model test/analysis time-history correlation for symmetrical drops	
(a) Horizontal velocity as a function of time	27
(b) Vertical velocity as a function of time	27
(c) Horizontal acceleration as a function of time	28
(d) Vertical acceleration as a function of time	28
A-7 Simulated-lunar-gravity test vehicle and related equipment at the LRC	28
B-1 Test summary of the LM landing gear	33
B-2 Landing-gear drop-test equipment	37
B-3 Landing gear configured for unsymmetrical drop test	37
B-4 Landing gear following drop into simulated lunar soil	37
C-1 Landing-gear uplock mechanism	48
C-2 Landing-gear deployment and downlock mechanism	
(a) Stowed position	48
(b) Down and locked position	48
C-3 Lunar-surface-sensing-probe-deployment mechanism	50
C-4 Lunar-surface-sensing-probe switch	50
C-5 Landing-gear footpad	51
C-6 Landing-gear-assembly test flow	52

APOLLO EXPERIENCE REPORT

LUNAR MODULE LANDING GEAR SUBSYSTEM

By William F. Rogers
Manned Spacecraft Center

SUMMARY

The development of the lunar module landing gear subsystem through the Apollo 11 lunar-landing mission is described in this report. Based on the design requirements, which must satisfy the structural, mechanical, and landing-performance constraints of the vehicle, the landing gear evolved from a fixed landing gear with five inverted tripod-type legs to a four-legged deployable landing gear.

Both extensive analyses and full-scale and model tests were undertaken to verify the design adequacy. The techniques developed for the landing-performance analyses served as a primary tool in the development of the subsystem hardware and in the prediction of the lunar module touchdown-performance capability. A major portion of the analyses was devoted to determining the performance adequacy of the landing gear for toppling stability and energy absorption. Landing-performance testing was used primarily to verify the analyses. The successful Apollo 11 lunar-landing mission provided the first opportunity for a complete flight test of the landing gear under both natural and induced environments.

INTRODUCTION

The landing of the lunar module (LM) on the surface of the moon is one of the more crucial events of the Apollo mission. During the critical seconds at touchdown, the LM landing system brings the vehicle to rest while preventing toppling, absorbing the landing-impact energy, and limiting loads induced into the LM structure. The landing-gear design is influenced significantly by the LM structural requirements, the LM control system, the lunar-surface topographical and soil characteristics, and the available stowage space. The landing gear also must provide a stable launch platform for lift-off of the ascent stage from the lunar surface.

The design and development of the LM landing gear subsystem hardware from the time of its conception through the Apollo 11 lunar-landing mission are presented. Also presented is the interaction of the landing gear with other LM subsystems. The specific design requirements for the landing-gear development are discussed, followed by the development history, a brief configuration description, a discussion of major problems,

and a summary of flight test results. Detailed information about the LM landing performance, the hardware development and testing, and the landing-gear configuration is given in appendixes A, B, and C, respectively.

DESIGN REQUIREMENTS AND CRITERIA

The landing gear subsystem hardware design requirements may be divided into three general categories — structural, mechanical, and landing performance. Structurally, the landing gear must withstand the loads and conditions imposed by the induced and natural environments defined in the technical specification (ref. 1) and in the report entitled "Design Criteria and Environments — LM" (ref. 2). The landing-gear strut loads must not exceed the LM structural-design requirements.

Mechanically, the landing gear must deploy properly and lock down while in lunar orbit. This is accomplished before the undocking of the LM from the command and service module (CSM). In the stowed position, the landing gear must physically clear the Saturn IVB (S-IVB) stage and the spacecraft/LM adapter (SLA) during the CSM/LM ejection maneuver, and landing-gear deployment must be controlled from within the LM cabin.

The landing gear must provide sufficient energy-absorption capability and adequate vehicle-toppling stability for the range of possible touchdown conditions and for the lunar-surface characteristics defined in the technical specification. On the lunar surface, the landing gear must prevent impact of the descent-stage base heat shield, fuel tanks, and plumbing with the lunar surface; however, the descent-engine skirt may contact the lunar surface. For the purpose of ascent-stage lift-off, the landing gear must allow the vehicle to come to rest so that the vehicle X-axis (fig. 1) does not exceed a specified tilt angle from the local vertical.

The landing gear must meet vehicle thermal-design requirements. Passive thermal control is used to maintain the landing-gear structural temperatures within the design range to ensure positive structural margins of safety and proper mechanical operation during deployment and landing. Included in this requirement is the necessity to control the temperature of the honeycomb-cartridge energy absorbers within specified limits to preclude large variations in crush load levels.

These items constitute the major design requirements and the general standards that were used in determining the adequacy of the landing-gear-subsystem design. The criticality of the landing gear is apparent. Structural or mechanical failure during touchdown could result in loss of life, depending on the mode of failure and whether or not any attempted ascent-stage abort during landing proved successful. Failure to achieve proper touchdown conditions or failure to land in an area of specified lunar-surface topography could result in an unstable landing or in structural failure because of overstroking a strut.

The design criteria most significant to the landing gear were those associated with the touchdown performance; specifically, the lunar-surface conditions and the vehicle initial conditions at touchdown. At the time the development of the LM landing gear was initiated, no detailed information was available concerning the lunar-surface

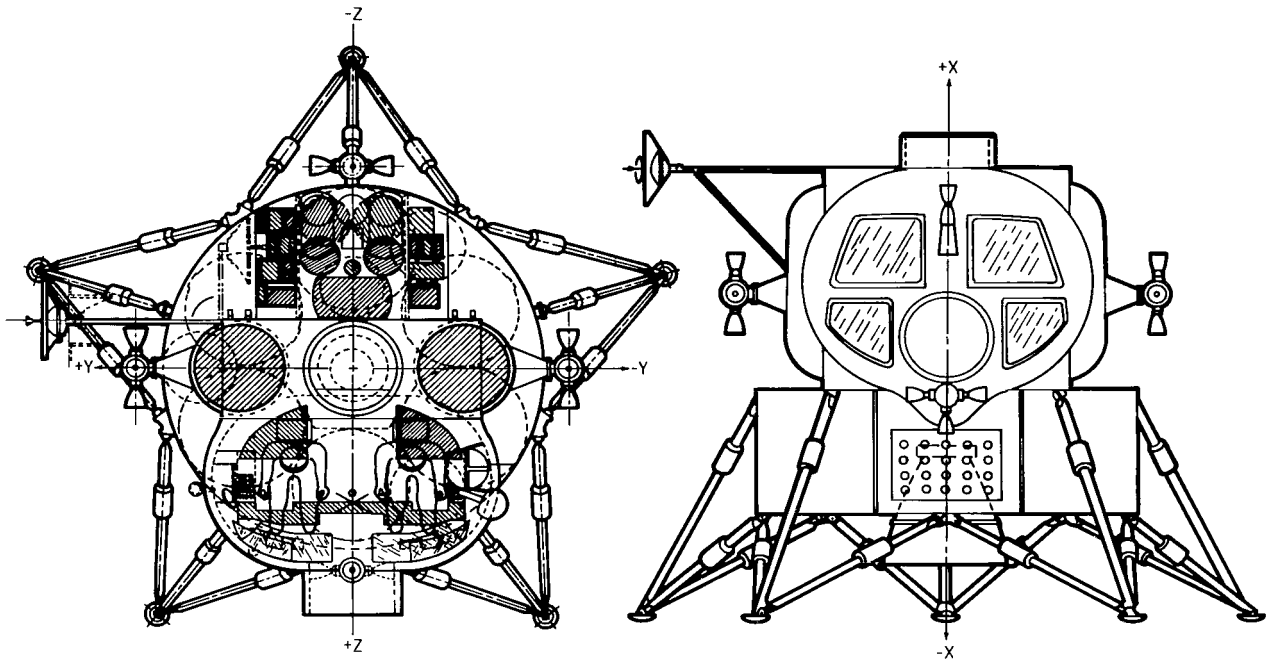


Figure 1. - The LM configuration (contractor technical proposal).

topography or soil characteristics; however, some preliminary data were available concerning vehicle touchdown conditions. A hypothetical lunar surface had to be assumed, for design purposes, to meet the Apollo Program schedule.

The lunar-surface specifications (refs. 1 and 2) contained both topographical and soil-property definitions. Topographical features consisted of a mean surface slope of 6° or less and an effective slope of 12° or less, including the effects of depressions or protuberances (or both) and footpad penetration. The assumption was made that, within the landing-gear footprint, the vertical distance from the top of the highest protuberance to the bottom of the lowest depression would be 24 inches or less. The soil bearing strength was such that a static load of 1.0 lb/in^2 would result in a penetration of 4 inches or less, and a dynamic load of 12 lb/in^2 would result in a penetration of 24 inches or less. The coefficient of sliding friction of the lunar surface was assumed to range from 0.4 to 1.0; however, complete constraint of the footpads could also be assumed. Data obtained from the NASA Surveyor and Lunar Orbiter Programs and the first Apollo lunar landing verified the adequacy of the lunar-surface specification. The bearing-strength assumptions were somewhat conservative in that the Apollo 11 landing indicated a 2 to 3 psi/in. lower boundary of bearing strength in the landing area. Post-flight analysis indicated that a coefficient of sliding friction of 0.4 was a realistic value.

Assumed initial conditions at touchdown (vehicle attitude, angular rates, and linear velocities) have varied during the course of the LM development. Initially, the touchdown velocities were specified as a 10-ft/sec maximum vertical velocity V_v and a 5-ft/sec maximum horizontal velocity V_h . This envelope was subsequently reduced

to a 4-ft/sec maximum horizontal velocity, based on updated simulation data. Later, the envelope was further reduced, as is discussed in the section entitled "Redesign of the 167-Inch-Tread-Radius Landing Gear." This final reduction resulted in an envelope where, for $V_v \leq 7$ ft/sec, $V_h = 4$ ft/sec; and, for 7 ft/sec $\leq V_v \leq 10$ ft/sec, $V_h = \frac{40}{3} - \frac{4}{3} V_v$ ft/sec. Further details of the lunar-surface description and initial conditions at touchdown are provided in appendix A.

For the purpose of structural design, the ultimate safety factor for the landing gear was 1.35, with an ultimate safety factor of 1.50 on all fittings. The 1.35 safety factor was based on the landing gear being a load-limited device; that is, the honeycomb energy absorbers used in the landing gear crush at predictable load levels, thereby absolutely limiting the loads that can be induced into the landing gear.

DEVELOPMENT HISTORY

The general design requirements discussed in the previous section have applied to the LM landing system since the decision in 1962 to use the lunar orbit rendezvous technique to accomplish a manned lunar landing. The LM configuration proposed by the contractor (fig. 1) consisted of a five-legged, fixed, inverted-tripod-type landing gear attached to a cylindrical descent stage. The five-legged landing gear was the lightest arrangement and provided the largest diameter base consistent with the space restrictions of the SLA without retraction. Configurations of four and six legs were also considered. The six-legged landing gear was approximately 40 pounds heavier than the selected arrangement and provided only a small increase in stability for the same diameter base. To provide the same stability as was available in the five-legged configuration, the four-legged landing gear required a larger diameter and retraction for stowage in the SLA.

Soon after the LM contract was awarded, the basic descent stage was changed from a cylindrical structure to a cruciform-type structure that could accommodate a four-legged landing gear more readily. The inverted-tripod-type landing gear, which consisted of a primary strut and two secondary struts joined near the footpad (fig. 1), is typical of the early configurations that were considered for both the cylindrical- and cruciform-shaped descent stages.

After selection of the four-legged landing gear, which required retraction for stowage because of the large landing-gear tread radius, many detailed inverted-tripod landing-gear leg designs were studied. Landing-gear tread radii ranged from 140 to 240 inches, with the tread radius defined as the distance from the vehicle longitudinal axis to the center of the landing-gear footpad.

The next major landing-gear design was the cantilever type in which the secondary struts are attached to the primary strut above the stroking portion (fig. 2). Studies conducted on cantilever-type landing gears with 160- to 180-inch tread radii resulted in the selection of a 167-inch-tread-radius landing gear as the final design. This selection was influenced significantly by the availability of stowage space. The major LM landing-gear configurations are summarized in table I.

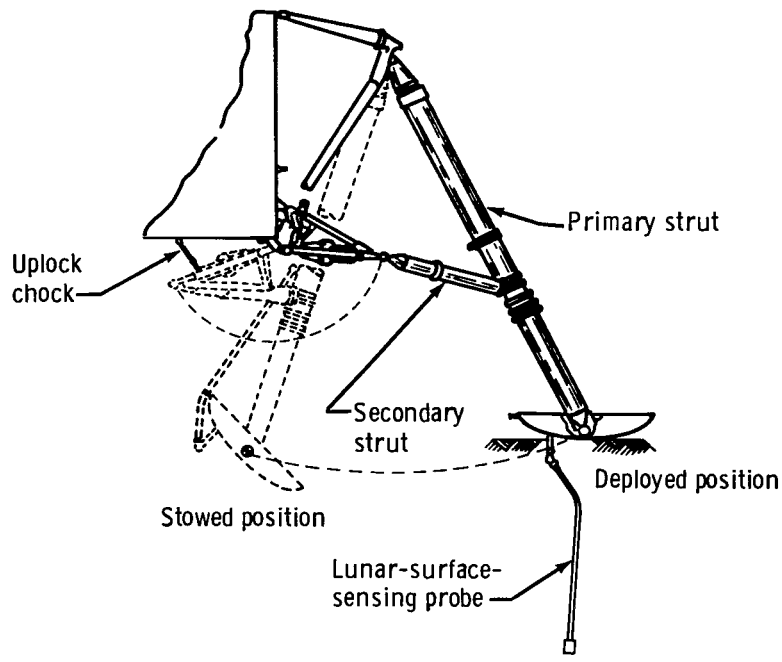


Figure 2. - Stowed and deployed positions of the landing gear.

TABLE I. - SIGNIFICANT LANDING-GEAR DESIGN CONCEPTS

Configuration	Tread radius, in.	Approximate date	Remarks
Tripod, 4 legs	--	Aug. 1962	Apollo statement of work configuration
Tripod, 5 legs	120	Sept. 1962	Contractor technical proposal
Tripod, 4 legs	140 to 240	Nov. 1963	--
Tripod, 4 legs	200	Nov. 1963	Lateral-retraction concept
Cantilever, 4 legs	160 to 180	Nov. 1963	Improved weight and performance
Cantilever, 4 legs	167	Dec. 1964	Optimum, based on performance analysis
Cantilever, 4 legs	167	July 1965	Redesigned landing gear with reduced strut loads and increased stroke capability



Design studies conducted on various landing-gear strut arrangements show that the cantilever-type landing gear has several advantages over the inverted-tripod arrangement. The cantilever-type landing gear weighs less, primarily because the secondary struts are much shorter than those in the inverted-tripod design. The shortening of the secondary struts and the simplification of the primary-strut-to-footpad attachment compensated for the increase in weight of the primary strut that was necessitated by the high bending loads encountered in the cantilever-type design. Because of light weight and relatively short length, the cantilever-type-landing-gear secondary struts are primarily axially loaded members that bend as a result of lateral inertial loading only. Another advantage of the cantilever-type design is that the location of the secondary struts minimizes interference problems in the vicinity of the footpad. Landing analyses indicated that the cantilever-type landing gear provided greater toppling stability than an inverted-tripod landing gear of the same tread radius, primarily because the cantilever-type landing gear provided a lower, and thus a more favorable, center-of-gravity (c. g.) location.

During the course of the landing-gear development, extensive testing was undertaken to investigate specific areas of concern, such as primary-strut bearings and honeycomb energy absorbers. During the development phases, testing was performed for all significant ground and flight environments. Certification testing, especially deployment tests in a thermal-vacuum environment and drop tests at design landing conditions, was accomplished, in accordance with Apollo Program test philosophy, on as complete a subsystem assembly as possible. Thus, landing-gear-assembly tests were used for the majority of the certification program. Development and design-verification testing was performed at both component and assembly levels. Model tests were conducted in support of the landing-performance analysis.

Landing dynamics was a major concern in the LM development. The LM touchdown-performance characteristics had to be compatible with a broadly defined lunar surface and with the LM control-system characteristics. Furthermore, the LM had to be capable of landing under conditions of zero visibility. Because of the difficulty in conducting meaningful and comprehensive full-scale landing-performance tests in the earth-gravity environment, extensive landing-dynamics analyses, using digital-computer simulations, were performed to evaluate the landing gear for both toppling stability and energy-absorption capability. The analyses were conducted concurrently with much of the structural and mechanical testing previously discussed. Results of both the development testing and the performance analyses were used to determine an optimum landing gear based on the design requirements. Analysis of the landing-gear performance also constituted a major portion of the flight certification. The landing performance and the hardware development and certification testing are discussed in detail in appendixes A and B, respectively.

CONFIGURATION DESCRIPTION

A sketch of the LM mounted in the SLA with the landing gear in the stowed position is shown in figure 3. The landing gear remains in the stowed position until the Apollo spacecraft is in lunar orbit. Deployment occurs during LM systems activation before powered descent to the lunar surface. The center of each LM footpad is 167.57 inches from the vehicle X-axis. A landing-gear leg assembly in both the stowed

and the deployed positions is shown in figure 2, and the major landing-gear components are shown in figure 4. An overall view of the final LM configuration with the landing gear deployed is shown in figure 5.

Each of the four separate landing-gear leg assemblies has energy-absorption capability in the single primary and two secondary struts. The deployment truss serves as a structural-mechanical assembly between the landing-gear struts and the descent-stage structure. Each landing-gear leg is retained in the stowed position by a titanium strap. When a pyrotechnic unlock device is fired, the titanium strap that is attached to the primary strut and the descent stage is severed, allowing the landing gear to be deployed and locked by mechanisms located on each side of the landing-gear leg assembly.

The primary strut (fig. 6) on each landing-gear leg assembly consists of a lower inner cylinder that fits into an upper outer cylinder to provide compression stroking (fig. 7) at touchdown. The strut is attached at the upper end (by a universal fitting) to

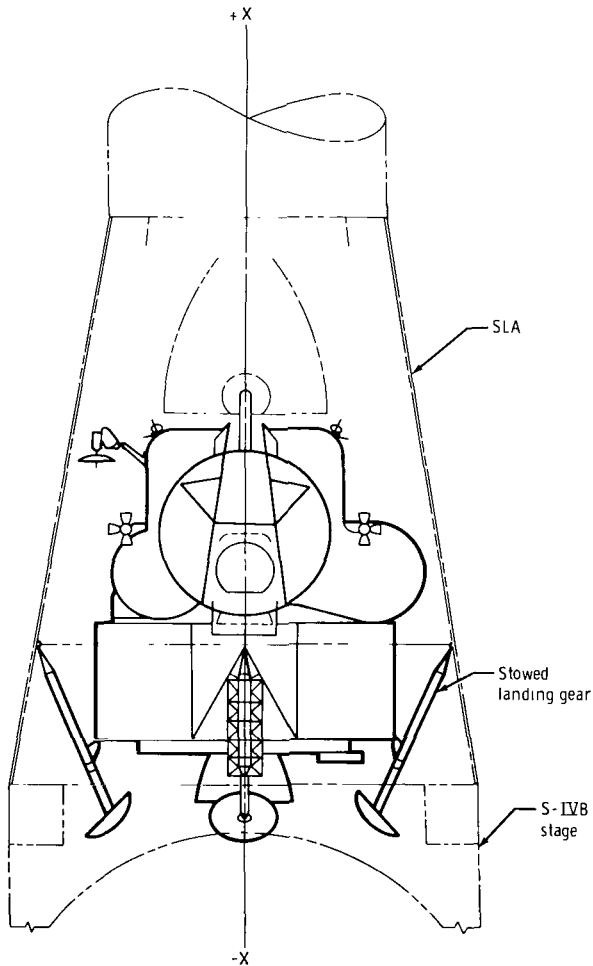


Figure 3.- The LM supported in the SLA.

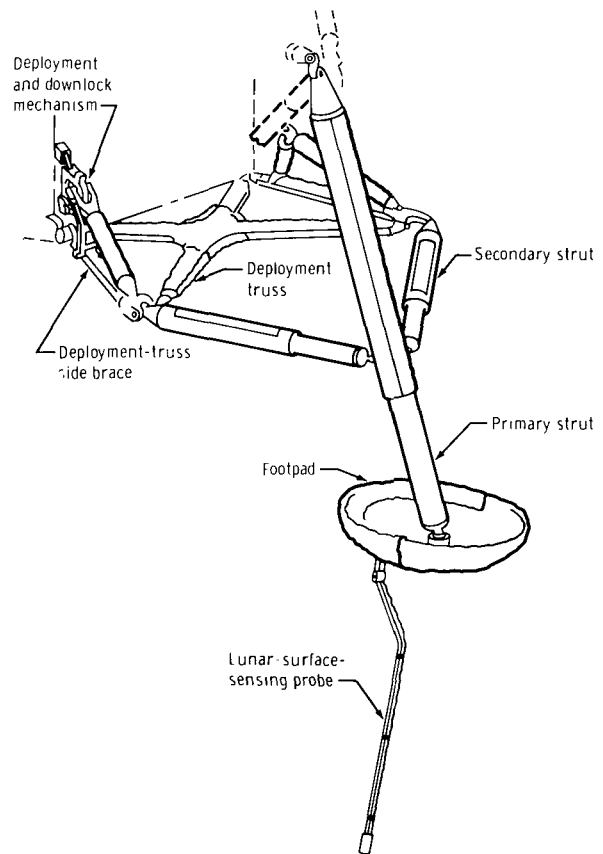


Figure 4.- The LM landing gear.

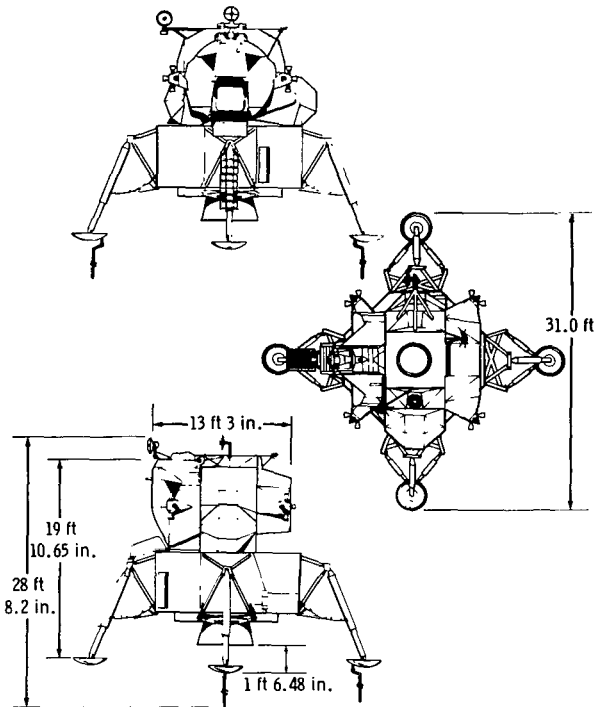


Figure 5. - Overall view of the LM with the landing gear deployed.

the LM descent-stage outrigger assembly. A footpad is attached to the lower end of the inner cylinder by a ball-joint fitting. The footpad, which is approximately 3 feet in diameter, is designed to support the LM on a 1.0-lb/in²-bearing-strength surface and to maintain functional capability after having impacted rocks or ledges during touchdown. The footpad is constructed of aluminum honeycomb bonded to machined aluminum face sheets. Attached to all footpads except the one on the forward landing gear (the plus-Z axis) is a 5.6-foot probe that is designed to sense lunar-surface proximity and to signal the LM pilot so that he can initiate descent-engine shutdown. The probe located on the forward landing gear was deleted because of a concern that the failed probe could interfere with crewmen descending the LM ladder.

The secondary struts (fig. 8) also have an inner and an outer cylinder. The

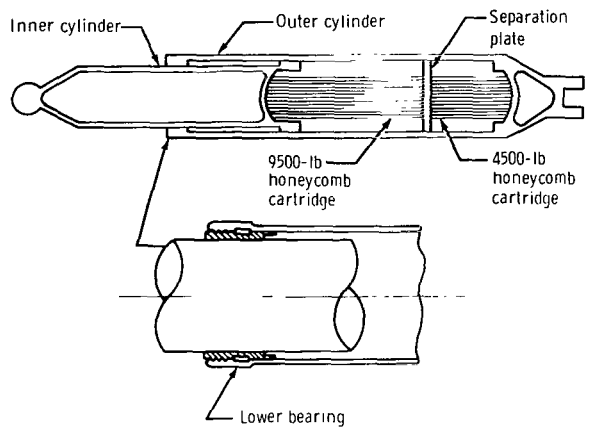


Figure 6. - Landing-gear primary strut.

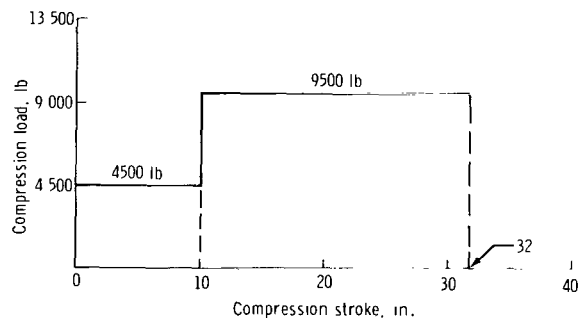


Figure 7. - Primary-strut compression load as a function of compression stroke.

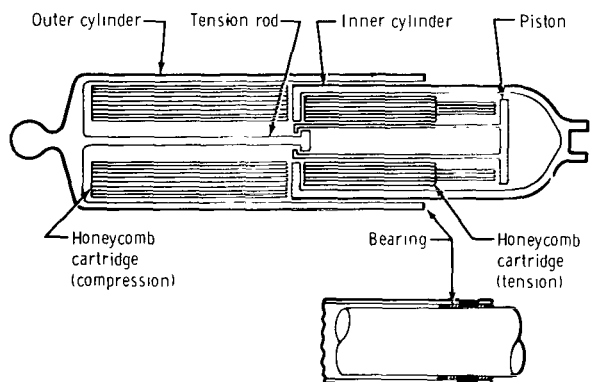


Figure 8. - Landing-gear secondary strut.

outer cylinder is connected to the primary strut by a ball-and-socket attachment, and the inner cylinder is attached to the deployment-truss assembly by a universal fitting. The secondary struts are capable of both tension and compression stroking (fig. 9). A detailed description of the flight-hardware components is contained in appendix C.

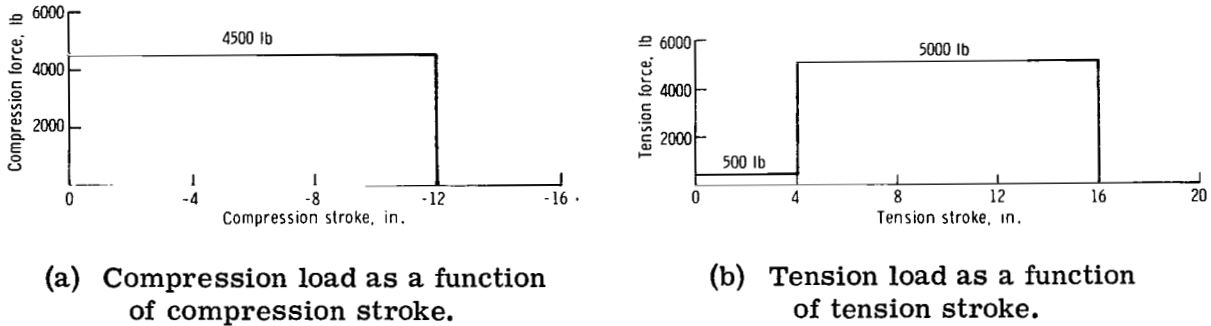


Figure 9. - Secondary-strut compression and tension loads.

MAJOR PROBLEMS

The major problems encountered during development of the landing-gear-subsystem hardware are discussed in this section. Some of these problems were solved by changes in the design criteria, and other problems were solved by hardware redesign. A summary of the landing-gear weight history and a brief discussion of the history of landing-gear failures during the Apollo Program are presented also.

Redesign of the 167-Inch-Tread-Radius Landing Gear

Early in 1965, a structural analysis of the landing gear and the primary LM structure revealed that the design load/stroke characteristics of the landing gear exceeded the vehicle structural capability. Also, vehicle-stability and strut-stroking requirements were not being achieved. These problems were identified as a result of increased vehicle weight, as well as a more refined analysis. To resolve the incompatibility, redesign of the LM structure or landing gear was necessary to reduce the loads imposed on the structure. A review of trade-off studies, showed the latter approach to be more desirable. An intensive effort was initiated to establish a landing-gear design with suitable load/stroke characteristics and to reduce the existing touchdown-velocity design envelope. The reassessment of the touchdown envelope necessitated a reevaluation of the touchdown-parameter statistical distributions associated with both manual and automatic landing techniques (ref. 3). The decision was made to consider an envelope acceptable if it could be demonstrated that the probability of the touchdown velocities falling within the envelope would exceed 0.9974 (the 3σ probability for a single, normally distributed random variable). Included in the study was an analysis to determine a lunar-surface-sensing-probe length that would ensure a high probability of engine-off landings within the touchdown-velocity design envelope.

As a result of the studies, the landing gear was redesigned to the load/stroke levels shown in figures 7 and 9. This design was designated the 167-inch (10-7-4) landing gear based on the maximum touchdown-velocity envelope assumed for the landing gear design (fig. 10). The actual limit boundaries for primary- and secondary-strut stroking and the actual stability boundary are also shown in figure 10. The vehicle orientation and surface conditions for critical stability and stroking are shown in figure 11. The reduced envelope was still well outside the 3σ touchdown-velocity envelope, which was based on piloted simulations. Besides the velocity-envelope revision, the attitude and attitude-rate criteria were revised, based on the simulation data. This change is an example of a reasonable criterion change, based on updated information, that alleviated a design problem.

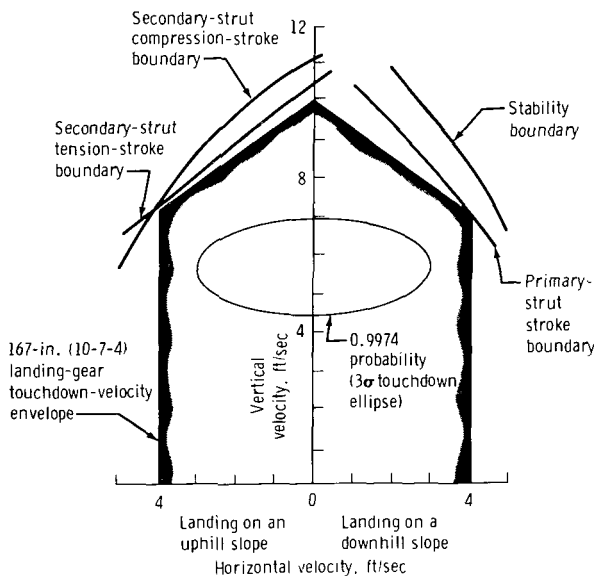


Figure 10. - Final-landing-gear landing performance.

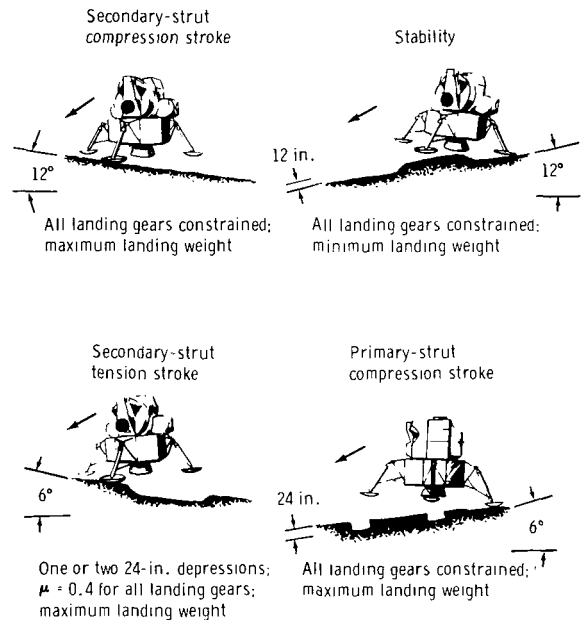


Figure 11. - Critical landing conditions.

Statistical Landing Performance

A major change in the treatment of the landing-performance-problem input parameters occurred as a result of the descent-engine thrust-decay time history. For design purposes, a thrust-decay time of approximately 0.5 second was used. A thrust decay of several seconds, which was an extremely destabilizing influence at touchdown, was evident in the actual descent-engine firing data. For worst-case combinations of parameters, the stability boundary lies well within both the design velocity envelope and the 3σ velocity envelope that had been derived from simulation data. Attempts to reduce the engine thrust-decay time by hardware changes were unsuccessful.

Another statistical analysis was performed to determine realistically the impact of the revised thrust-decay time. At the time this analysis was performed, detailed Lunar Orbiter photographic data of the lunar surface were available. To make the

analysis as realistic as possible, a statistical description of the lunar surface, which consisted of general surface slopes and surface protuberances and depressions, was derived from Lunar Orbiter photography. Statistical descriptions of potential Apollo landing sites were formulated and, based on general surface slope, the most severe site was chosen for the analysis. This analysis, which was used to certify the adequacy of the LM landing performance, constituted a criterion change because of the method of combining design parameters.

Another factor that influenced the landing-performance analysis was the desire of the Apollo 11 (LM-5) crewmen to have the option of thrusting the descent engine until the footpads had touched down, rather than initiating engine shutdown following lunar-surface-probe contact. This option resulted in additional analysis, and statistical results were obtained for both the "probe" mode and the "pad" mode type of LM landing.

The probe mode is the primary procedure for LM touchdown and consists of descent-engine shutdown initiation following probe contact but before footpad contact. The pad mode is considered a backup landing mode in which engine thrust is terminated following footpad contact. Touchdown performance was predicted for both landing procedures. The touchdown-velocity ellipse for each mode and pertinent information on other initial conditions at touchdown are shown in figure 12. The data used in the analysis are compared with the Apollo 11 (LM-5) results, which are discussed in more detail in the section entitled "Apollo 11 Flight-Test Results."

The estimated probability factor for achieving a stable configuration using the probe mode is 0.967. If slopes greater than 12° are removed arbitrarily from the calculations, the probability factor is increased to 0.998. For the pad mode, the probability of a stable landing anywhere in the landing ellipse is 0.986. If stroking is considered, the probability of using less than the available stroke for a landing in either mode is 0.999.

Although these probabilities are based on a Monte Carlo statistical analysis, considerable conservatism is involved, as previously noted. The stability analysis is based entirely on constrained-footpad-type landings. Footpad sliding is not considered in calculating toppling stability. For the calculations of stroking, the energy-absorption characteristics of the lunar soil are not considered. Furthermore, the statistical surface description is based on the Apollo site that has the most severe topographic relief of the Apollo landing sites originally considered. No crew selectivity was assumed to be involved in choosing the touchdown point within the landing site.

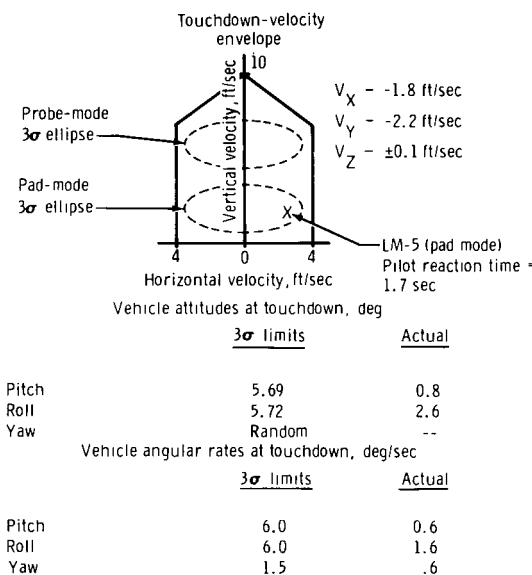


Figure 12. - Apollo 11 attitude and motion touchdown conditions.

Thermal Insulation

Landing-gear thermal-insulation design is based on several requirements. Landing-gear temperatures must be maintained at or below design levels to ensure positive structural margins of safety and proper mechanical operation during deployment and landing. Temperature control of the honeycomb energy absorbers within specified limits is necessary to ensure that the crush loads will be within proper levels.

Based on these requirements, an estimated 8.0 pounds of thermal paint was allotted to landing-gear thermal control early in the development program. The weight history of the landing-gear thermal insulation is shown in table II. As thermal testing and analysis progressed, it became apparent that 8.0 pounds of thermal paint were totally inadequate for landing-gear thermal protection. Additional insulation had to be provided because of the effects of LM reaction control system (RCS) plume impingement. The impingement from the RCS plume adversely affected the structural temperatures and the temperature of the honeycomb energy absorbers in the primary and secondary struts. Landing-performance analysis, for which the energy-absorber load levels that are temperature dependent were used, showed considerable degradation in landing-gear performance for worst-case combinations of honeycomb temperatures and landing conditions. The outcome of this investigation was the addition of thermal-insulation blankets to the main structural members of the landing gear. The thermal-insulation weight (table II) was increased to 29.4 pounds for the Apollo 9 LM (LM-3) and Apollo 10 LM (LM-4), which were the first two LM flight articles to have landing gears.

TABLE II. - LANDING-GEAR THERMAL-INSULATION WEIGHT HISTORY

Approximate date	Weight, lb	Remarks
Nov. 1964	8	Thermal-paint estimate; no thermal blankets or plume shielding defined
Mar. 1967	^a 22	RCS plume-impingement requirement
Feb. 1969	29.4	Apollo 9 mission, actual
May 1969	29.4	Apollo 10 mission, actual
June 1969	68.4	Apollo 11 mission, actual; weight change caused by thrust until footpad contact and increased heating rates on landing gear

^a Approximately.

Another significant thermal-design problem related to the landing gear was the effect of descent-engine-plume heating. A few months before the flight of Apollo 11, data from scale-model shock-tube tests indicated that heating rates on the landing gear were much higher than previously had been considered for design. This increase resulted in an extensive effort to design additional thermal insulation for the landing gear and to perform structural and mechanical tests on the affected hardware.

At approximately the time the problem of excessive heating rates was identified, the LM flight crew expressed a desire to have the option of using either the pad mode or the probe mode. Inclusion of the pad mode resulted in even higher predicted heating rates for the landing gear. Consequently, the Apollo 11 landing-gear thermal-insulation weight was increased 39 pounds over that of Apollo 10. A more refined analysis allowed reduction of the landing-gear-insulation weight on subsequent vehicles.

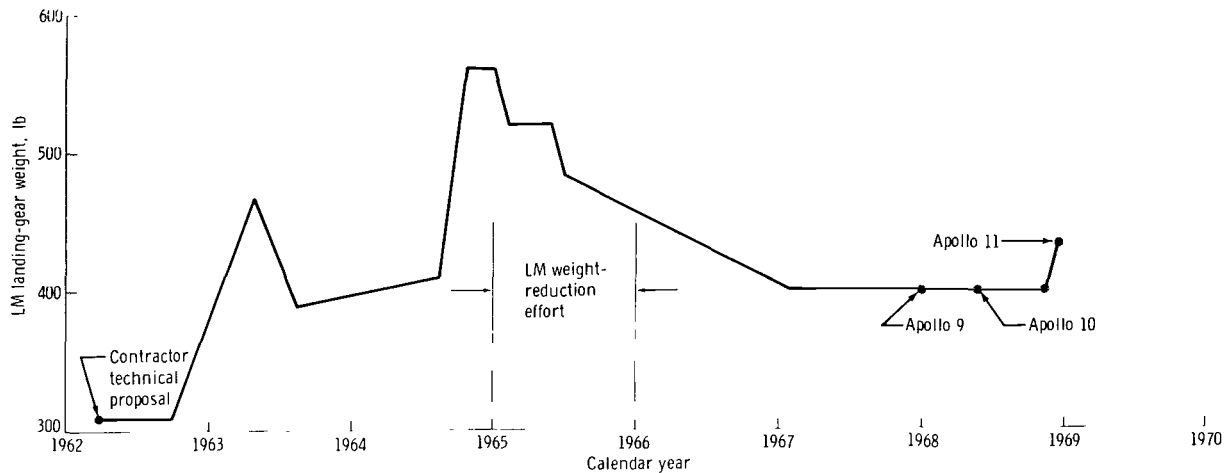
Weight Summary

Summaries of the LM and the LM landing-gear-subsystem weight histories are presented in figure 13. The final landing-gear weight was considerably higher than originally predicted. One reason for the significant increase was the decision to use a deployable four-legged landing gear instead of the proposed fixed five-legged arrangement. As the total LM weight was increased, the landing-gear weight was also increased.



(a) The LM touchdown weight history.

Figure 13. - The LM weight history.



(b) The LM landing-gear weight history.

Figure 13. - Concluded.

During the latter half of 1965 and the first half of 1966, a concerted effort was made to decrease the overall LM weight. A landing-gear weight decrease of approximately 75 pounds was accomplished primarily in two ways. The landing-gear redesign to decrease structural loads (discussed in appendix A) also decreased landing-gear loads, which resulted in a substantial weight savings. Second, approximately 40 pounds were saved through general redesign efforts, such as replacing machined struts having riveted end fittings with struts having integral fittings. No further weight changes were made until the requirements for additional thermal insulation on the Apollo 11 LM caused a significant increase. The thermal-insulation design was refined following the Apollo 11 mission to a final landing-gear weight of approximately 456 pounds, or less than 3 percent of the vehicle landing weight. A summary of the Apollo 11 landing-gear major-component weights is given in table III.

TABLE III. - APOLLO 11 LANDING-GEAR-COMPONENT WEIGHT SUMMARY

Component	Weight, lb
Primary struts ^a	217.3
Secondary struts ^a	68.8
Footpads	44.9
Deployment truss and deployment mechanisms	80.4
Lunar-surface-sensing probes	6.7
Thermal insulation	68.4
Total	486.5

^aTotal honeycomb-energy-absorber weight in all struts is approximately 61 pounds.

Failure History

Although landing-gear hardware failures were not a major problem, a discussion of the types of failures, the causes, and the corrective actions is pertinent. A history of the landing-gear failures and where they occurred is given in table IV. Failures of the lunar-surface-sensing-probe switch subassembly are listed separately because this was the most troublesome component during the development.

TABLE IV. - LANDING-GEAR FAILURE HISTORY

Place of failure	Number of failures, year and quarter															
	1966				1967				1968				1969			
	1	2	3	4	1	2	3	4	1	2	3	4	1	2	3	4
Lunar-surface-sensing-probe switch assembly																
Vendor				5				3	4			5		3	1	
Contractor facility																
Launch site												1				
Landing-gear assembly																
Vendor				1				1								
Contractor facility					2		1		1							
Launch site																

The failures listed in table IV occurred during certification testing and acceptance and ground-checkout testing. The probe-switch failures were about evenly divided between certification and acceptance tests. After a reed switch inside the switch subassembly had been identified as a weak component, fabrication techniques for the switch assembly were improved, and the failure rate decreased significantly. During preflight checkout, the probe-switch mechanism was also subject to inadvertent mechanical actuation into the latched position. For this reason, a final visual check of the switches is performed shortly before launch. A latch in the switch electrical circuitry (designed to ensure that the lunar-contact lights in the cabin remain illuminated following probe contact), rather than the mechanical latch, would have eliminated this problem.

Included in the landing-gear-assembly failures are two landing-gear deployment failures, one during certification and the other during vehicle checkout. No landing-gear failures of any type, structural, mechanical, thermal, or touchdown performance, have occurred during flight. Differences between the certified configuration and the flight hardware are listed in appendix B, with the rationale for the adequacy of the flight hardware. Also listed in appendix B are all certification-level tests performed during the course of the landing-gear development.

APOLLO 11 FLIGHT-TEST RESULTS

The initial landing of an LM on the lunar surface constituted the first complete flight test of the landing-gear hardware. Landing-gear deployment in space had been demonstrated on two previous manned LM flights, Apollo 9 and 10. Before the Apollo 11 mission, LM landing performance and landing-gear functional operation had been demonstrated by analysis and by extensive ground tests. During these tests, the landing gear was exposed to all significant flight environments, including vehicle drop tests under simulated lunar-gravity conditions.

The touchdown of the Apollo 11 LM on the lunar surface occurred at very low vertical and horizontal velocities. Landing occurred in the pad mode. An overall view of the LM resting on the lunar surface is shown in figure 14, and a closeup view of the minus-Z footpad is shown in figure 15. From these photographs, it was determined that the landing occurred on a relatively flat, smooth surface and that negligible landing-gear stroking occurred.

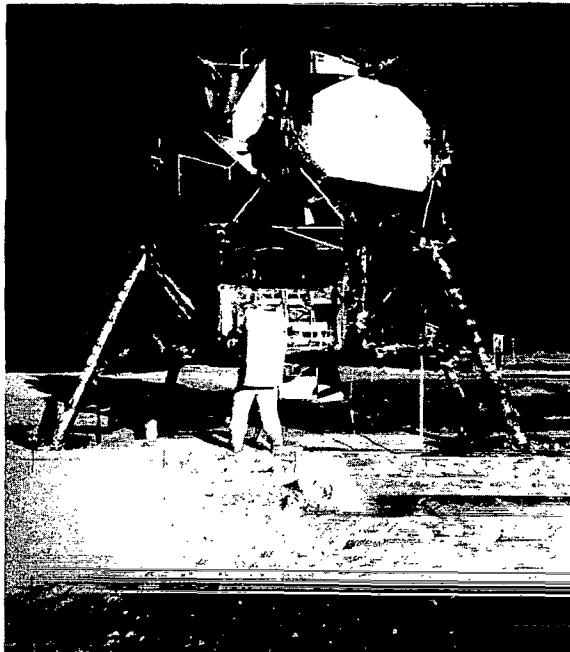


Figure 14. - Apollo 11 LM (LM-5)
on the lunar surface.

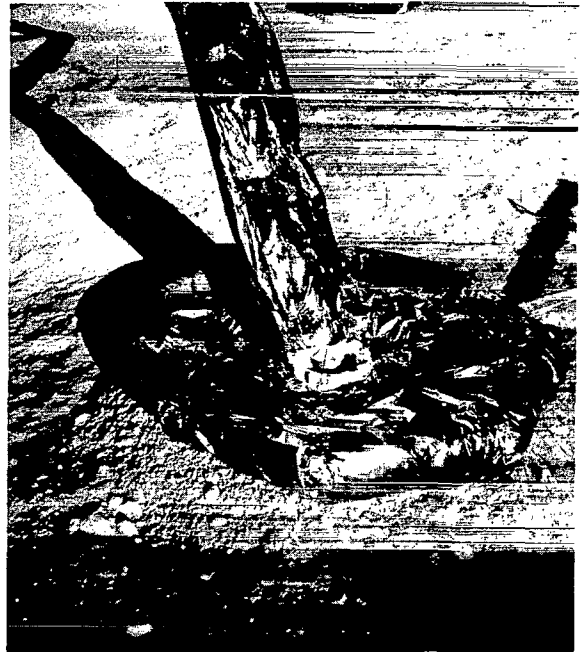
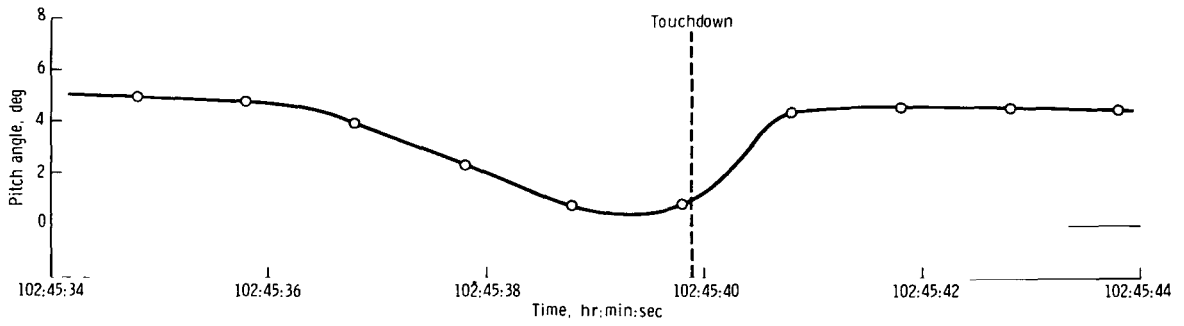
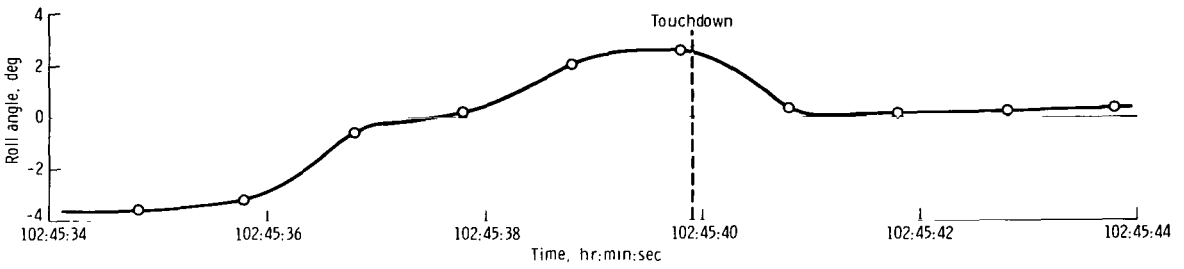


Figure 15. - Apollo 11 LM (LM-5)
minus-Z (aft) footpad.

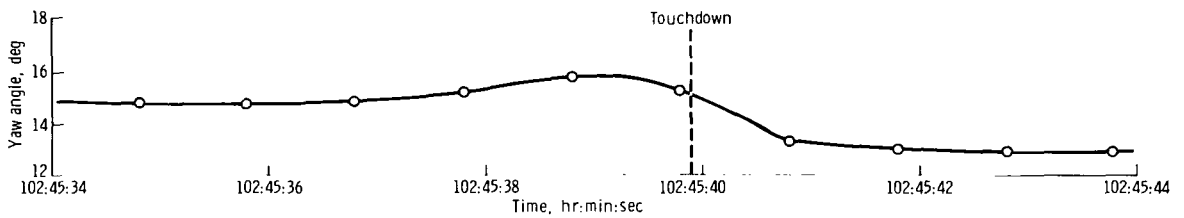
The landing occurred with negligible plus-Z velocity, a minus-Y velocity of approximately 2.1 ft/sec, and a minus-X velocity of approximately 1.7 ft/sec. Vehicle angular-rate transients (fig. 16) indicate that the right- and forward-landing-gear legs touched almost simultaneously, which resulted in a roll-left and pitch-up vehicle motion. The touchdown conditions, which were obtained from attitude-rate data and



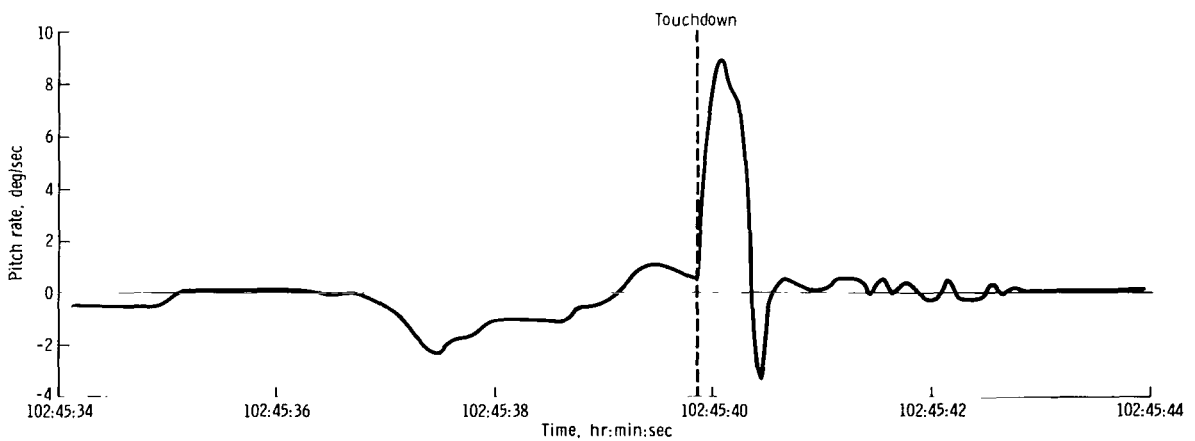
(a) Pitch angle as a function of time.



(b) Roll angle as a function of time.

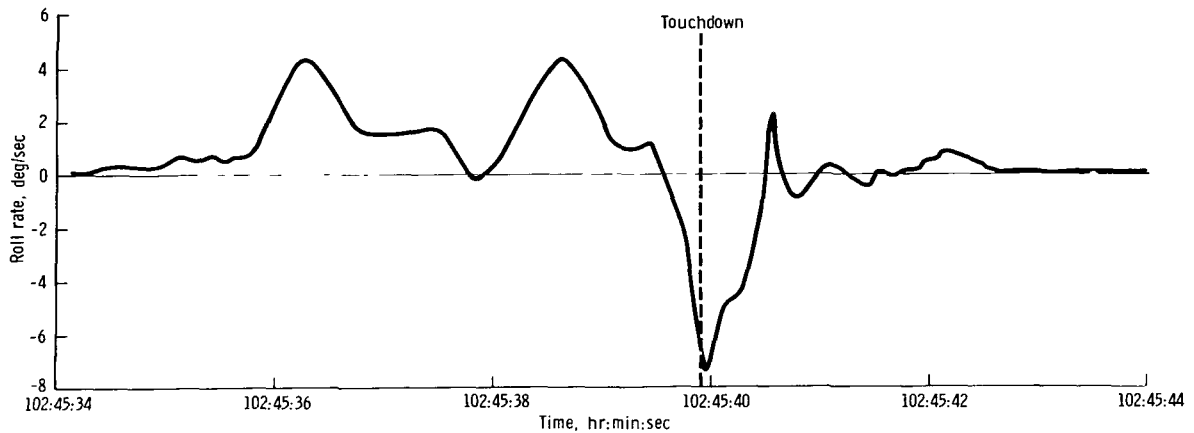


(c) Yaw angle as a function of time.

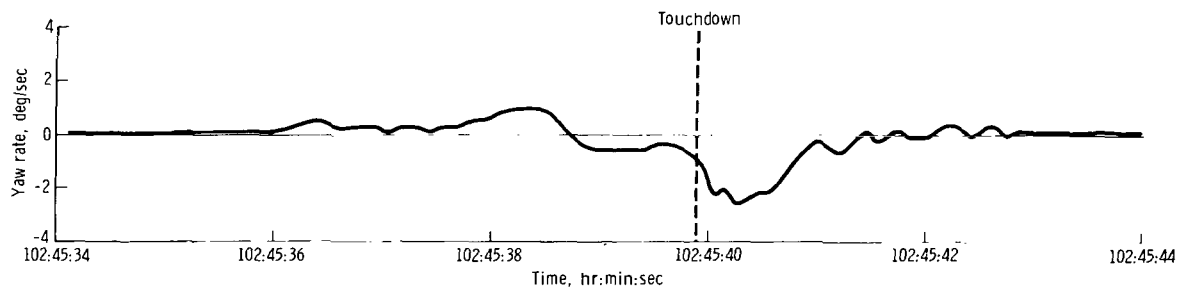


(d) Pitch rate as a function of time.

Figure 16. - Apollo 11 (LM-5) attitudes and attitude rates at touchdown.



(e) Roll rate as a function of time.



(f) Yaw rate as a function of time.

Figure 16. - Concluded.

integration of accelerometer data, were verified qualitatively by the positions of the lunar-surface-sensing probes and by lunar-soil buildup around the footpads. The probe boom in figure 14 is nearly vertical on the inboard side of the minus-Y footpad, which indicates a component of velocity in the minus-Y direction. Soil is apparently built up on the outboard side of the pad, which indicates a lateral velocity in that direction. The probe position and the lunar-soil disturbance produced by the minus-Z landing-gear assembly (fig. 16(a)) indicate a lateral velocity in the minus-Y direction. The soil disturbance on the minus-Y side of the minus-Z footpad is shown in greater detail in figure 15. The soil disturbance around the plus-Y landing-gear assembly indicates a minus-Y velocity of this leg at touchdown because the probe on the plus-Y leg was on the outboard side and soil was piled inboard of the pad.

The crewmen reported no sensation of toppling instability during touchdown. A postflight simulation of the landing dynamics indicated a maximum footpad penetration of 0.5 to 1.5 inches and a footpad slide distance of 18 to 22 inches. Results of postflight-simulation predictions of strut stroking have been compared with estimates derived from the landing-gear photographs. Primary-strut stroking was estimated by comparing photographs of the LM after touchdown with photographs of the landing gear before the flight. The conclusion was that little or no stroking of the primary struts occurred.

Because the inner cylinder of the secondary struts has a rigid Inconel thermal shield, stroking could be estimated by scaling the dimensions of the struts in the photographs. At least a 0.25-inch uncertainty existed in this measurement because of the manner in which the thermal shield is attached to the inner cylinder. The stroking was estimated by scaling the distance from the end of the Inconel thermal cuff to the edge of the outer-cylinder end cap near the primary-strut juncture. A scale factor was obtained by measuring the diameter of the strut end cap in the photograph. Where necessary, the measurements were corrected for the strut axis not being normal to the camera view. The stroke estimates are listed in table V. Where there was more than one photograph of a strut from which the stroke could be estimated, a comparison is shown. The strokes that were derived by analysis of the photographs are estimated to be accurate within 1.0 inch. Secondary-strut tension stroking was as much as 4 inches. Even though the primary strut is designed for a maximum 32-inch stroke, no primary-strut stroking was recorded on Apollo 11.

TABLE V. - APOLLO 11 (LM-5) STRUT-STROKE ESTIMATES

Strut	Average photographic estimate, in.	Simulation estimate, in.
Plus-Z, primary	0	0
Plus-Z, right	--	.2
Plus-Z, left	^a 4.0	^a 3.6
Minus-Z, primary	0	0
Minus-Z, right	^a 2.5	^a 3.2
Minus-Z, left	^a 4.5	^a .2
Plus-Y, primary	0	0
Plus-Y, right	^a 2.8	^a 3.4
Plus-Y, left	^a .5	^a 1.0
Minus-Y, primary	0	0
Minus-Y, right	^a 3.2	^a 1.4
Minus-Y, left	0	^a 1.4

^aTension.

The engine-skirt clearance values measured from the photographs and the values predicted from postflight simulations were found to be in excellent agreement. The distance between the lunar surface and the engine-nozzle exit is estimated from the photographs to be 13.5 inches. Based on landing simulations, a clearance of 13.8 inches was predicted. The skirt clearance for an LM resting on a flat surface with no struts stroked is 19 inches. The decreased ground clearance is further evidence to support the stroking analysis, which indicated a small amount of secondary-strut tension stroking that resulted in lowering the vehicle. The Apollo 11 LM appeared to be resting on a relatively flat surface. The engine skirt is shown in figure 17, and a slight amount of soil erosion caused by the engine exhaust is visible beneath the skirt.

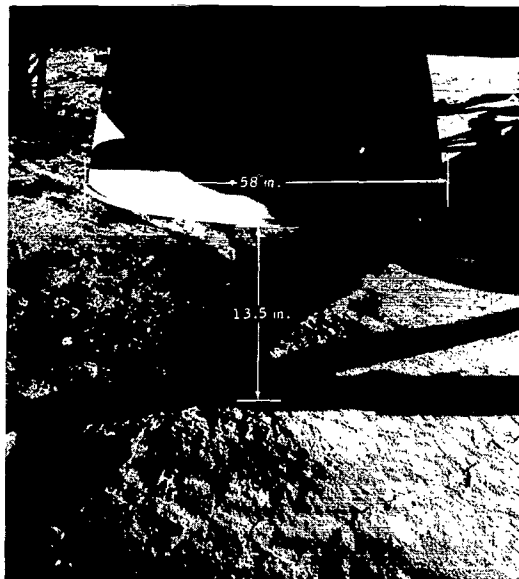


Figure 17. - Apollo 11 (LM-5) descent-engine skirt.

CONCLUDING REMARKS

Development of the lunar module landing-gear hardware started in mid-1962 and continued until mid-1969, when the first manned lunar landing occurred. During this period, development problems were encountered and successfully solved. At no time did the availability of landing-gear hardware jeopardize the Apollo Program schedule.

One of the worthwhile outgrowths of the landing-gear program has been the development of techniques of landing-performance analysis. The lunar module landing-dynamics analytical computer program has been used as a prime tool in the development of the subsystem hardware and in the prediction of the lunar module touchdown performance. Landing-performance testing, which was extremely complex and expensive, was used primarily to verify the analysis. Final certification of the lunar module landing-performance adequacy was based solely on analysis. The computer program developed for the lunar module landing analyses can be adapted readily for future manned and unmanned spacecraft landing-analysis studies.

A review of the hardware indicates that the lunar-surface-sensing-probe switch, although adequate, was troublesome. A latching mechanism in the electrical circuitry, rather than the mechanical latch that was used, could have prevented some of the problems encountered.

A brief summary of the overall landing-gear performance may be stated as follows.

1. Structural: All components and mechanisms have been test demonstrated or determined by analysis to equal or exceed the design requirements.

2. Mechanical: All mechanisms have been functionally test demonstrated to be adequate under lunar-mission environments.

3. Landing performance: For the Apollo landing sites, the energy-absorption and toppling-stability capabilities are adequate. The probability of never attaining maximum strut stroking is greater than 0.999, and the probability of attaining a stable landing on a slope of 12° or less is 0.998.

Manned Spacecraft Center
National Aeronautics and Space Administration
Houston, Texas, January 6, 1972
914-13-20-13-72

REFERENCES

1. Anon.: Contract Technical Specification for Lunar Module Systems. Rept. LSP-470-1D, Grumman Aircraft Engineering Corp., Oct. 1, 1968.
2. Anon.: Design Criteria and Environments — LM. Rept. LED-520-1 H, Grumman Aircraft Engineering Corp., Oct. 19, 1970.
3. Anon.: IIB LEM Lunar Landing Simulation Studies. Rept. LED-470-5, Grumman Aircraft Engineering Corp., Feb. 18, 1966.

APPENDIX A

LANDING PERFORMANCE OF THE LM

Landing dynamics was a major concern during the development of the LM. The LM touchdown-performance characteristics must be compatible with both a broadly defined lunar surface and the LM control-system characteristics. Furthermore, the LM must be capable of landing under conditions of zero visibility.

Because of the difficulty in conducting meaningful and comprehensive full-scale landing-performance tests in the earth-gravity environment, an extensive landing-dynamics analysis, in which digital-computer simulations were used, was the primary tool for proving the adequacy of the landing gear for both toppling stability and landing-gear energy-absorption capability. This analysis was conducted concurrently with much of the structural and mechanical testing. Results of both the development testing and the performance analysis were used to develop an optimum landing gear that fulfilled the design requirements. Analysis of the landing-gear performance also constituted a major portion of the flightworthiness certification.

Landing-performance tests were limited to 1/6-scale-model tests and to planar-type full-scale landing-performance tests in a simulated lunar-gravity environment at the NASA Langley Research Center (LRC). Despite the relatively few landing-dynamics tests conducted, a high degree of confidence in the predictions exists, based on the analysis. Independent analyses performed by the prime contractor and by NASA were correlated with each other and with the 1/6-scale and full-scale test data available. The analysis/test correlation performed to verify the mathematical model is shown in figure A-1.

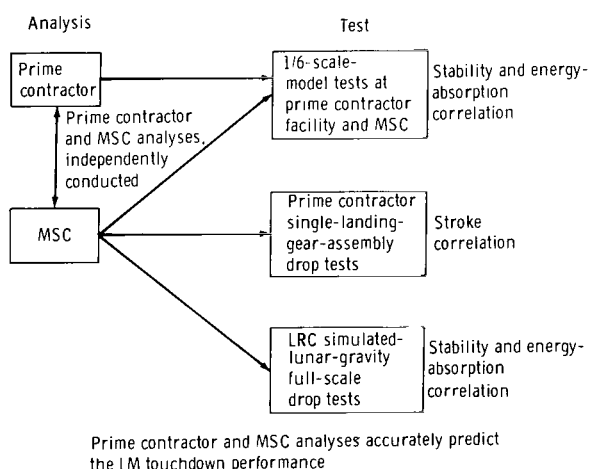


Figure A-1. - Validation of touchdown-analysis mathematical model.

This appendix contains a detailed discussion of the LM landing-dynamics analysis and discussions of the lunar surface and the touchdown conditions, two extremely important aspects of the analysis. Details of the model tests used to verify the analysis are discussed, and, finally, the LM touchdown-performance history and present capability are discussed.

LANDING-DYNAMICS ANALYSIS

For the purpose of studying various landing-gear designs, a simplified planar-type landing-dynamics analysis was used; however, for a detailed analysis and evaluation of landing-gear mechanisms and for

providing design information for landing-load determinations and landing-gear-performance predictions, a three-dimensional landing-dynamics computer program was required. The following description of the LM landing-dynamics computer program is typical of the analyses used for landing studies. Detailed descriptions of the prime contractor analysis may be found in references A-1 and A-2, and a description of the NASA Manned Spacecraft Center analysis is given in reference A-3.

Two basic requirements of the analysis were that it must realistically model the geometry and loading of the individual landing-gear members and that it must be capable of accommodating a wide variety of lunar-surface conditions. For landing-dynamics studies, the LM, except for the landing gear, is considered to be a rigid body. An unsprung mass represents the mass of the footpad and the primary strut. The primary and secondary struts stroke axially and absorb energy according to the load/stroke curves shown in figures 7 and 9. The struts are considered to be rigid in flexure for the purpose of determining the landing-gear geometry that results from stroking. Strut elasticity is introduced to the extent that it affects the overall vehicle motion.

The energy absorption that results when a strut is stroked axially is incorporated in the model by assuming an elastic-plastic load/stroke characteristic. Energy, which is represented by the elastic portion of the curve, is released back into the system because of the axial elasticity of the strut. For the secondary struts, bending loads caused by transverse inertia are assumed to be negligible; therefore, the secondary struts are only loaded axially. The secondary-strut side loads cause sizable primary-strut bearing loads that must be accounted for in the stroking analysis. The load/stroke curve for each strut may vary because of manufacturing tolerances, strut-stroking velocity, and honeycomb temperatures. For this reason, the analysis enables different honeycomb characteristics to be assigned to each strut.

The lunar surface at the touchdown point may have a general slope as well as various combinations of protuberances and depressions. Because of the surface characteristics, a footpad may be subjected to sliding-friction forces or to full constraint. Surface forces normal to the footpad are assumed to be elastic-plastic. In addition, footpad loads caused by lateral crushing are represented for cases in which the footpad slides into a rigid obstacle. Combinations of footpad conditions can be represented in a single landing simulation.

Other significant effects are included in the analysis. Control moments caused by RCS thrusting may be included. Because it is possible for the descent-engine nozzle extension to impact the lunar surface, the load/stroke characteristics of the crushable nozzle are included. Nozzle energy-absorption characteristics are based on tests of full-scale engine skirts. In addition to the descent-engine thrust, considerable forces may be exerted by the interaction of the descent-engine exhaust plume with the lunar surface, which causes surface-effect forces on the base of the vehicle. Significant engine thrust may occur with the nozzle close to the lunar surface because of the long thrust-decay time or because the pilot may choose to touch down with the engine on. A landing on top of a large protuberance or mound would place the nozzle close to the surface. With the nozzle thrusting close to the surface, a thrust-amplification effect occurs. This effect has a sizable influence on the LM toppling-stability characteristics and is accounted for in the analysis.



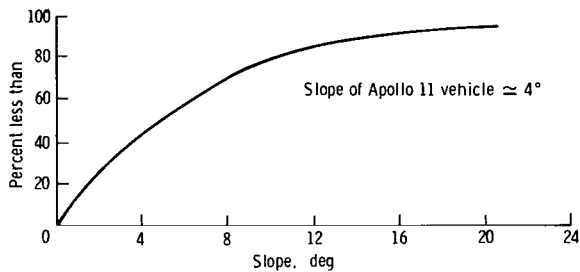
The vehicle c. g. has six degrees of freedom, three translational and three rotational. In addition, each footpad has three translational degrees of freedom. A total of 18 nonlinear, second-order, simultaneous differential equations of motion must be integrated to describe the vehicle dynamics. Results of a landing simulation include time histories of the rigid-body vehicle positions, velocities, and accelerations. In addition, footpad motion, strut loads, and strut strokes are obtained. The toppling stability of the vehicle is also monitored. The vehicle is assumed to be stable neutrally if the vehicle tips to a point at which the vehicle c. g. coincides with the vertical plane that passes through the center of any two adjacent footpads. The vehicle tipping velocity and the distance between the vehicle mass center and the vertical plane are measures of the vehicle stability. If the vehicle stability and strut strokes are known, landing-gear performance evaluations can be made.

During the early stages of the landing-gear analysis, it was discovered that certain types of landings tend to be critical with respect to the vehicle stability or the stroking of a particular strut. Although these particular landings could not be judged to be worst-case landings, they were the worst cases found and were considered to be good indicators of the adequacy of the particular landing-gear configuration being studied. These landing cases were called control runs and were used extensively for evaluation of the landing-gear designs. As analysis work continued, a more realistic look at landing performance was desired, which resulted in several statistical studies. The basic analysis for the statistical studies was the same as that used for the discrete analyses. Statistical representations of the lunar surface, spacecraft initial conditions at touchdown, and pertinent parameters (such as descent-engine thrust-decay time histories) were used in the statistical analyses.

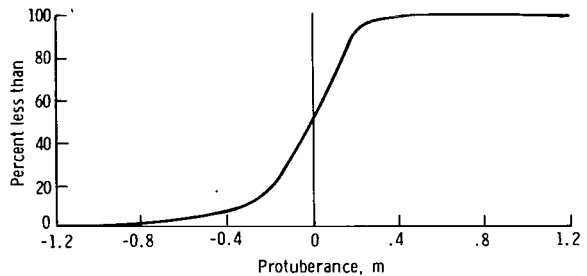
LUNAR-SURFACE DESCRIPTION

To design an LM landing system, the surface on which the LM is to touch down must be defined. At the time the contract to produce a lunar-landing vehicle was awarded, only meager information was available concerning the lunar-surface topographical features and soil characteristics. Therefore, a surface had to be assumed that not only was reasonable but also was broad enough to accommodate a wide range of actual landing sites. A specification of the lunar surface was formulated, and, based on this specification, the landing gear was designed and manufactured.

The original lunar-surface description (refs. 1 and 2) consisted of the topographical and soil-property features defined in the section of this report entitled "Design Requirements and Criteria." A comprehensive soil-mechanics study (ref. A-4) was conducted in support of the LM landing analysis. Statistical descriptions were also formulated for various statistical studies of landing performance and for landing-load analysis. The statistical description used most extensively was based on topographical data from the Lunar Orbiter photography of the most severe Apollo landing site (fig. A-2). With the exception of one study, no attempt was made to establish statistical values for soil properties. In general, the footpads were considered to be fully constrained for all studies, except for secondary-strut tension stroking for which a low friction coefficient is a crucial parameter. Although the specification defined 0.4 as the minimum value for the friction coefficient, lower values were investigated in secondary-strut strokeout studies.



(a) Slope profile.



(b) Protuberance profile.

Figure A-2. - Lunar-surface description.

TOUCHDOWN CONDITIONS

In addition to the lunar-surface characteristics, the initial conditions at footpad contact are extremely important factors in the LM landing-dynamics analysis. The initial conditions of vehicle attitude, angular rates, and linear velocities at touchdown have varied to some extent during the course of the LM development. However, the following final-specification values were used for most of the deterministic-analysis work (ref. 3).

The angle between the LM X-axis and the local gravity vector must be $\leq 6^\circ$, with yaw attitudes being a random variable. The angular-rate vector, which is based on the combined effects of the angular rate about each body axis, must be less than 2 deg/sec. The final-velocity envelope is defined by the vertical descent velocity V_v and the horizontal velocity V_h . For $V_v \leq 7$ ft/sec, $V_h = 4$ ft/sec; and, for 7 ft/sec $\leq V_v \leq 10$ ft/sec, $V_h = \frac{40}{3} - \frac{4}{3} V_v$ ft/sec. For the statistical landing analyses, data from fixed-base pilot simulations of LM touchdown were used.

LANDING-DYNAMICS MODEL TESTS

Because of the heavy emphasis placed on analysis for demonstrating LM landing-performance adequacy, some means of verifying the basic analysis was required. To accomplish this, extensive 1/6-scale-model and full-scale-model test programs were undertaken, and the results were correlated with the results of the landing-dynamics analysis.

One-Sixth-Scale-Model Tests

One-sixth-scale-model tests were performed at the prime contractor facility and at the MSC. The results of the correlation of the model tests at the prime contractor facility with the analysis are presented in reference A-5. In general, the correlations

for vehicle stability and landing-gear energy absorption were considered to be the most important. Instrumentation of the models permitted comparisons of acceleration, velocity, and displacement time histories with the analytical results.

By using the technique of dynamic scaling, a model was designed that could be tested in the earth-gravity environment. The resulting model was constructed to a 1/6-dimensional scale and a $(1/6)^3$ mass scale, and the ratio of the model touchdown velocities to the touchdown velocities of the full-scale LM was 1.0. The model had the desirable characteristics of being untethered, of having a convenient size and weight for handling, and of having easily obtainable mass properties. Scale parts, including landing-gear energy absorbers, generally presented no great manufacturing problem. However, the fabrication of reliable 1/6-scale honeycomb cartridges was an initial problem. The small number of cells in the scale cartridges caused cartridge instability during stroking, which resulted in poor load/stroke characteristics. The final test cartridges were handmade and contained a sufficient number of cells to provide repeatable load/stroke characteristics.

Because the models were constructed early in the LM development program, they did not represent later LM detailed landing-gear and mass characteristics. However, the purpose of the model test program was to correlate results with the results of an analytical touchdown analysis; therefore, no attempt was made to keep the models continuously updated to LM vehicle changes. A view of the LM model is shown in figure A-3, and the contractor drop-test facility is shown in figure A-4. The facility enabled simulation of initial conditions at touchdown, including both planar- and three-dimensional-type landings. In addition, the landing surface could include protuberances, depressions, and slopes as required, and a rigid surface or various types of soil could be used for the simulation.

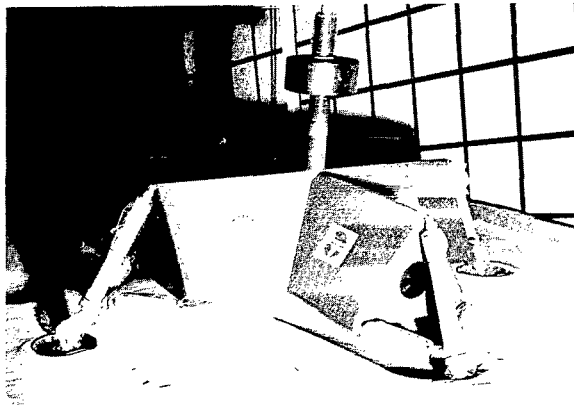


Figure A-3. - One-sixth-scale drop-test model.

Examples of the comparison of 1/6-scale-model test results with the results of the analysis are shown in figures A-5 and A-6, which are taken from reference A-5. A comparison of the stability boundaries obtained for a particular drop condition at various vertical and horizontal velocities is shown in figure A-5. A comparison of the time histories of both rigid-body acceleration and velocity is shown in figure A-6. These results are typical of the reasonably good correlation that was obtained between model and analysis results. Good correlation was also obtained between predicted and measured strut strokes. Similar results were obtained with 1/6-scale-model tests at the MSC.

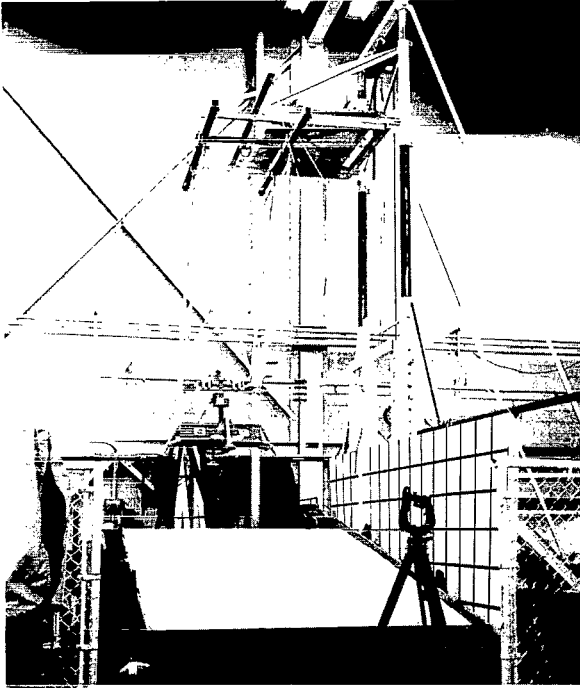


Figure A-4. - One-sixth-scale model and drop-test equipment at the prime contractor facility.

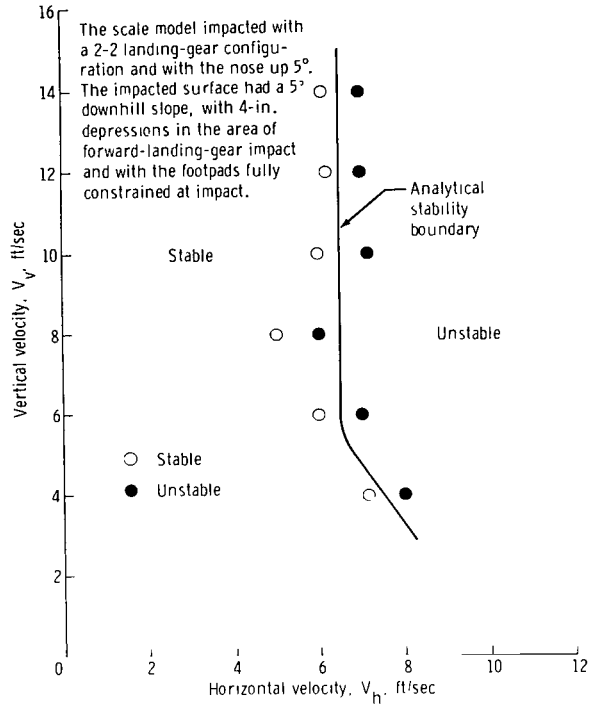
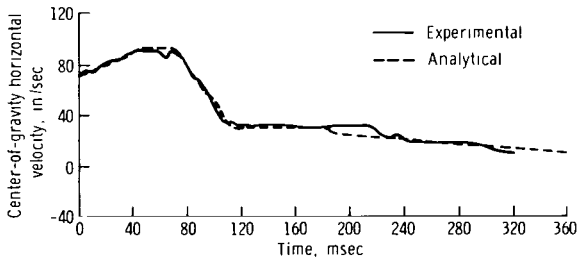
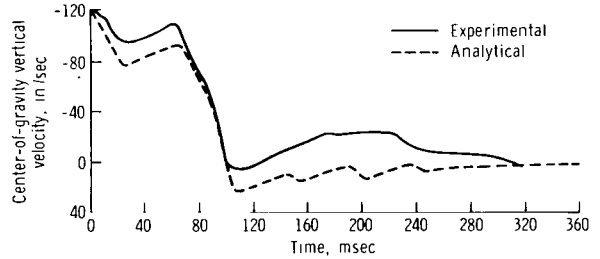


Figure A-5. - One-sixth-scale-model test/analysis gross correlation for symmetrical drops.

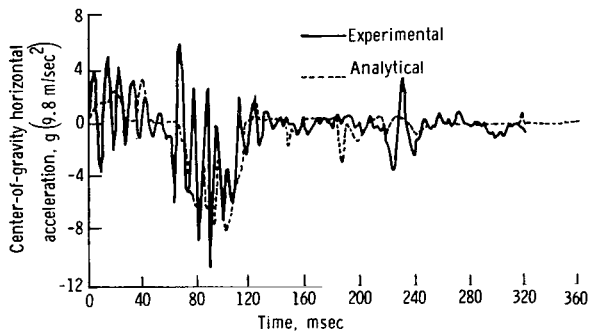


(a) Horizontal velocity as a function of time.

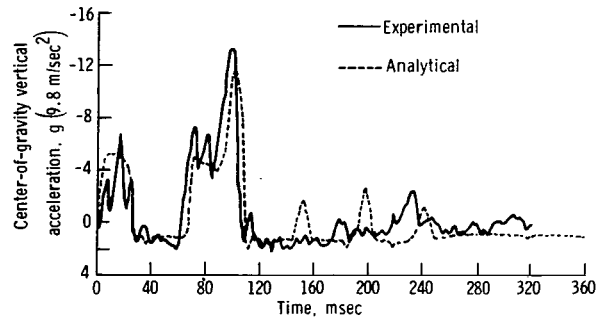


(b) Vertical velocity as a function of time.

Figure A-6. - One-sixth-scale-model test/analysis time-history correlation for symmetrical drops.



(c) Horizontal acceleration as a function of time.



(d) Vertical acceleration as a function of time.

Figure A-6. - Concluded.

Full-Scale-Model Tests

In addition to the 1/6-scale-model tests, a series of tests was performed using a full-scale mass representation of the LM and a preproduction 167-inch-tread-radius cantilever-type landing gear. These tests were performed at LRC in a simulated lunar-gravity environment. The lunar gravity was simulated by dropping the model, which was suspended from cables, onto an inclined plane. The plane was tilted at an angle that provided one-sixth earth gravity normal to the vehicle landing surface. The remaining weight of the vehicle was nullified by supporting cables. Twenty-one drop tests were conducted in the series using the vehicle shown in figure A-7. The lunar-gravity-simulation touchdown surface is also shown in figure A-7. Results of the LRC test program and some comparisons of the test data with analytical predictions are presented in references A-6 and A-7.

Although these tests were restricted to planar-type landings, much useful information was obtained relative to the functional characteristics of the landing gear. The tests provided increased confidence in the LM-landing-gear functional operation and also provided test data for stability and energy-absorption evaluation.

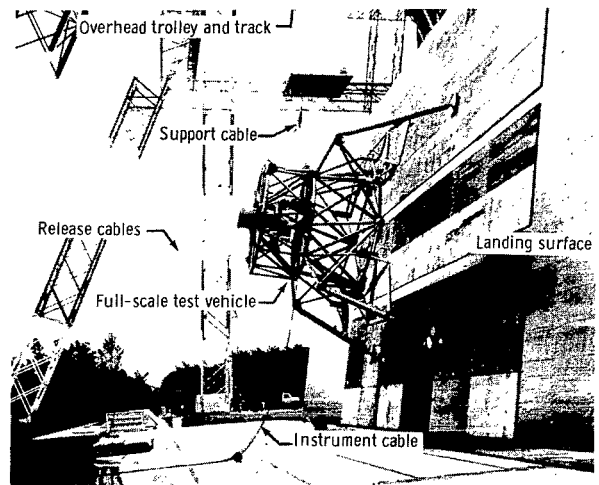


Figure A-7. - Simulated-lunar-gravity test vehicle and related equipment at the LRC.

Consideration was given to conducting simulated-lunar-gravity tests at the prime contractor facility. These tests would permit unsymmetrical-type landing simulations; however, this kind of test was not conducted because the high cost would not justify the limited amount of information that would have been gained. Numerous development problems encountered during the design of the lunar-gravity-simulation portion of the test equipment also contributed to the decision to cancel these tests.

LANDING PERFORMANCE

The landing-performance analysis has been used extensively as a tool in the LM landing-gear design and performance evaluation. Landing-gear performance studies may be roughly divided into two categories: the deterministic- or worst-case-type analysis that was used for landing-gear design and early performance evaluations, and the statistical or Monte Carlo analysis that was used to predict the probability of a successful landing.

Deterministic Landing Analysis

In initial design studies, only landings in which the vehicle c. g. motion was planar were considered. Two landing-gear orientations were considered for symmetrical landings. The orientation with one leading landing gear, two side landing gears, and one trailing landing gear was designated the 1-2-1 case. The case with two landing gears leading and two trailing is called the 2-2 case. In general, for symmetrical landings, the 2-2 case is stability critical, and the 1-2-1 case is critical for primary-strut energy-absorption requirements.

As the analysis was refined, unsymmetrical-type landings were considered. Two of the more important parameters in unsymmetrical-type landings are yaw attitude and the vehicle flight-path angle. Typical unsymmetrical landing performances, which are based on a set of critical landings, are summarized in figures 10 and 11. The vehicle orientation and the lunar-surface conditions for critical stability, primary-strut stroke, secondary-strut compression stroke, and secondary-strut tension stroke are shown in figure 11. The stability and secondary-strut stroke boundaries are critical for unsymmetrical landings. The primary-strut stroke is critical for the symmetrical 1-2-1 landing case. The velocity envelope shown in figure 10 was the envelope chosen for design purposes in mid-1965 and is described in the section of this report entitled "Statistical Landing Performance."

Based on an LM touchdown weight of 16 000 earth pounds, the kinetic energy involved in a landing with a 10-ft/sec vertical velocity would be approximately 26 000 ft-lb. An additional energy contribution is provided by the potential energy. For example, 8000 ft-lb of potential energy could be involved as a result of a vehicle c. g. displacement of 3 feet from a combination of landing-gear stroking, vehicle touchdown attitude, and surface topography. One landing-gear assembly, which consists of all energy-absorption capability in the primary strut and the two secondary struts, is equivalent to approximately 30 870 ft-lb (21 200 ft-lb in the primary strut and 9670 ft-lb in the secondary struts (5170 ft-lb in tension and 4500 ft-lb in compression)). The distribution of

energy absorption for each landing-gear leg depends on many factors during the landing, but the value for the energy-absorption capability of each landing gear corresponds approximately to the design requirement for total energy absorption.

Statistical Landing Analysis

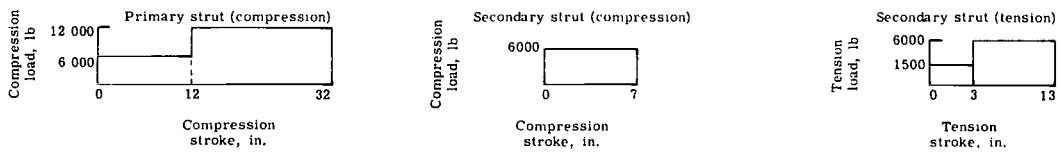
The analytical landing performance was based on combining touchdown initial conditions and lunar-surface conditions in an effort to obtain worst-case simulations. Because of the large number of parameters involved, it was not practical to establish with absolute certainty the worst possible combinations of parameters; therefore, to show that the worst-case design conditions constituted an extremely severe basis for performance evaluation, a statistical analysis of the landing-performance problem was conducted.

For the initial statistical analysis, the four critical measurements of landing-gear performance (stability, primary-strut stroke, secondary-strut tension stroke, and secondary-strut compression stroke) were considered separately (refs. A-3 and A-8). This approach was taken to produce a conservative statistical analysis, because parameters that are conservative for one performance measurement are not necessarily conservative for another. For example, a low value for the footpad/soil friction coefficient may be critical for secondary-strut tension strokeout but not for vehicle stability, where full footpad constraint is the critical parameter. A summary of the major landing-gear performance analyses that were completed before the Apollo 11 lunar landing in July 1969 is contained in table A-I.

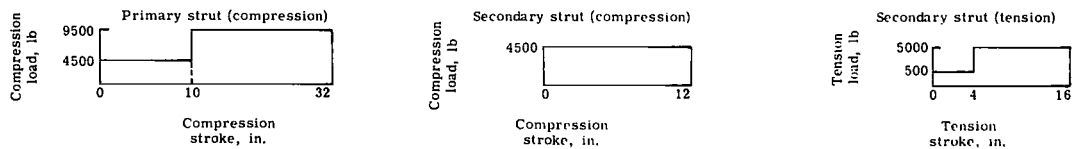
TABLE A-1. - LANDING-PERFORMANCE HISTORY OF THE LM

Date	Type of analysis	Stability	Primary strut (comparison)	Secondary strut (compression)	Secondary strut (tension)
Sept. 1965	Deterministic, for critical-landing cases ^a				
Oct. 1965	Deterministic, for critical-landing cases ^b				
June 1967	Statistical ^b	A 0.99999 probability of a stable landing	A 0.99999 probability of using less than a 32-in. stroke	A 0.99999 probability of using less than an 8.5-in. stroke	A 0.99999 probability of using less than a 16-in. stroke
Aug. 1968	Worst case, with new thrust decay ^b		No significant change from June 1967 results	No significant change from June 1967 results	No significant change from June 1967 results
Dec. 1968	Statistical, with new thrust decay ^b	A 0.967 probability for any touchdown in the landing sites; a 0.998 probability for a landing on any slope less than 12°	A 0.999 probability of using less than a 30-in. stroke	A 0.999 probability of using less than a 12-in. stroke	A 0.999 probability of using less than a 16-in. stroke
Apr. 1969	Worst-case thrust until footpad contact ^b		Stroke margin for this procedure exceeds that for procedure of engine shutdown at probe contact.	Stroke margin for this procedure exceeds that for procedure of engine shutdown at probe contact.	Stroke margin for this procedure exceeds that for procedure of engine shutdown at probe contact.
June 1969	Statistical thrust until footpad contact ^b	A 0.986 probability for any touchdown in the landing site (based on 300 landings)	A 0.995 probability of using less than a 12.0-in. stroke	A 0.995 probability of using less than a 5.0-in. stroke	A 0.996 probability of using less than a 5.0-in. stroke

^aOld 167-in. -tread-radius landing-gear load/stroke characteristics:



^bThe 167-in. -tread-radius (10-7-4) landing-gear load/stroke characteristics:



REFERENCES

- A-1. Hilderman, Richard A; Mueller, William H. ; and Mantus, Morton: Landing Dynamics of the Lunar Excursion Module. J. Spacecraft Rockets, vol. 3, no. 10, Oct. 1966, pp. 1484-1489.
- A-2. Anon. : Landing Dynamics of the Lunar Module (Performance Characteristics). Rept. LED-520-17, Grumman Aircraft Engineering Corp. , June 15, 1967.
- A-3. Zupp, George A. , Jr. ; and Doiron, Harold H. : A Mathematical Procedure for Predicting the Touchdown Dynamics of a Soft-Landing Vehicle. NASA TN D-7045, 1971.
- A-4. Anon. : Lunar Module (LM) Soil Mechanics Study. Final Report. Rept. AM-68-1, Energy Controls Division, Bendix Corp. , May 1, 1968.
- A-5. Anon. : Landing Dynamics of the Lunar Excursion Module (1/6 Scale Model III Test-Analysis Correlation). Rept. LED-520-12, Grumman Aircraft Engineering Corp. , May 16, 1966.
- A-6. Blanchard, Ulysse J. : Full-Scale Dynamic Landing-Impact Investigation of a Prototype Lunar Module Landing Gear. NASA TN D-5029, 1969.
- A-7. Blanchard, Ulysse J. : Evaluation of a Full-Scale Lunar-Gravity Simulator by Comparison of Landing-Impact Tests of a Full-Scale and a 1/6-Scale Model. NASA TN D-4474, 1968.
- A-8. Anon. : Landing Dynamics of the Lunar Module (Performance Characteristics Including Descent Engine Thrust Decay Effects). Rept. LED-520-53, Grumman Aircraft Engineering Corp. , Apr. 16, 1969.

APPENDIX B

HARDWARE DEVELOPMENT AND CERTIFICATION TESTING

The LM landing-gear design evolved from many studies during the period from mid-1962 until late 1964 when the 167-inch-tread-radius cantilever-type landing gear was chosen as the basic design. During the course of the landing-gear development, extensive testing was undertaken to investigate specific areas of concern, such as primary-strut bearings and honeycomb energy absorbers. Included in this appendix is a discussion of the component- and assembly-level testing of the landing gear during both the development and certification-test phases of the program.

TEST-HISTORY SUMMARY

A test history of the component, assembly, and model testing performed in support of the landing-gear development and certification is shown in figure B-1. The LM flight dates are shown at the bottom of the figure. The test dates are approximate in some cases, but the chart gives an overall indication of the degree of testing performed. As can be seen, many honeycomb-cartridge development tests were performed, and many 1/6-scale-model drop tests were conducted to support the landing-analysis verification.

Testing was performed for all significant ground and flight environments during the development. In accordance with the Apollo Program test philosophy, certification testing was accomplished on as complete a subsystem assembly as possible. Thus, landing-gear-assembly tests were used for the major portion of the certification program. Development and design-verification testing was performed at both component and assembly levels. Model tests in support of the landing analysis are discussed in the section of appendix A entitled "Landing-Dynamics Model Tests."

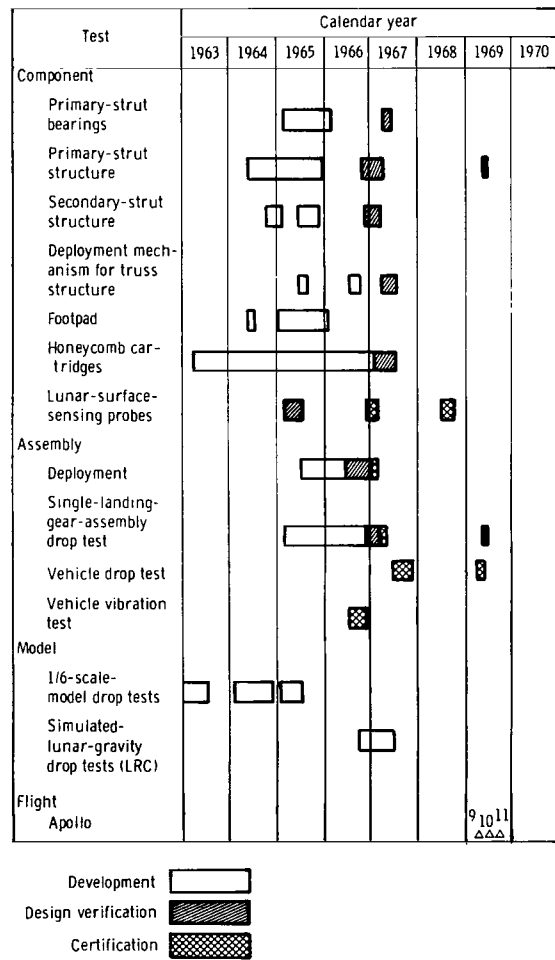


Figure B-1. - Test summary of the LM landing gear.

DEPLOYMENT TESTS

Extensive landing-gear deployment tests were conducted, beginning with the 160-inch-tread-radius landing-gear design. Tests were conducted in ambient, salt-fog, and thermal-vacuum environments, with the majority conducted under ambient conditions. Deployment testing was generally conducted with the landing-gear-assembly axis of deployment in the vertical position; that is, the primary-strut longitudinal axis was perpendicular to the gravity vector. To minimize gravity effects, a cable was attached to the landing gear near its c. g.

Energy requirements for landing-gear deployment were generally determined by testing. Because of the complexity of the landing-gear motions during deployment and because of the difficulty of accurately estimating friction loads at the bearing joints, the deployment energy requirements were only grossly predicted by analysis. Simulated-zero-gravity deployment tests were used as a design tool to verify the deployment energy requirements and to test the deployment-mechanism hardware concepts.

During early deployment testing, much design information was obtained about the deployment-mechanism functionality and deployment time. Strut loads were measured to determine the magnitudes of the loads induced by the deployment shock. Honeycomb-cartridge lengths in the secondary strut were measured to determine if any honeycomb crushing occurred as a result of the inertial forces produced by deployment. Loads induced into the LM structure by deployment were measured also. Quantitative data from later tests performed on flight-type hardware consisted primarily of deployment-time information. This information was used to verify that changes to the landing-gear thermal insulation had not adversely affected deployment and to verify the accuracy of the landing-gear checkout tests at the prime contractor facility and at the launch site. The landing-gear-assembly deployment tests (development, design verification, and certification), beginning with initial ground-test hardware and concluding with flight-vehicle checkout and flight-test results, are summarized in table B-I. All deployment-test failures and the cause of each failure are also summarized. As indicated in table B-I, almost 250 individual landing-gear deployments have been made through the Apollo 11 mission. Detailed information on the development, design-verification, and certification tests may be found in references B-1 to B-9.

Two deployment failures occurred during certification and checkout testing: one during a thermal-vacuum certification test and the other during factory checkout of the Apollo 9 landing gear. The certification-test failure resulted from the use of an improper lubricant in the deployment springs during a thermal-vacuum test at a temperature of -150° F. In this instance, the landing gear deployed and locked, but not within the specified time. With the correct lubricant on the springs, operation was nominal. The deployment failure on the Apollo 9 landing gear during factory checkout resulted from two deficiencies: thermal-insulation interference with a deployment-truss rotating joint and marginal energy in both deployment springs of the failed landing gear. The insulation was redesigned in the vicinity of the deployment joints, the required spring energy was increased, and more rigid acceptance-test requirements were imposed on the deployment-spring assemblies. Component tests of the leaf-type deployment spring consisted primarily of functional tests under various environments and of fatigue tests (ref. B-10).

TABLE B-I. - LANDING-GEAR DEPLOYMENT-TEST SUMMARY

Type of test	Configuration	Test objectives	Environment	Number of deployments	Remarks
Development	A 160-in. -tread-radius landing gear with coil deployment springs	To evaluate functionally To determine loads into structure and into landing-gear struts To determine effects on secondary-strut honeycomb	Simulated zero gravity	59	In 54 ambient tests, one failure to lock down from a partially deployed position when one deployment spring was used; in five salt-fog tests, one failure to deploy when one deployment spring only was used
Development	A 160-in. -tread-radius landing gear with leaf-type deployment	To evaluate functionally To evaluate new type spring	Simulated zero gravity	41	One failure to lock down from a partially deployed position when 16 percent of nominal torque was used
Design verification	A 167-in. -tread-radius landing gear (10-7-4)	To establish preflight checkout criteria To determine effects of thermal insulation	Earth gravity; ambient	24	One failure to fully deploy with one spring removed; one failure to deploy when a truss pivot fitting was intentionally jammed
Design verification	A 167-in. -tread-radius landing gear (10-7-4)	To evaluate functionally To determine effects of thermal insulation	Simulated zero gravity; ambient	49	--
Certification	A 167-in. -tread-radius landing gear (10-7-4)	To evaluate functionally	Simulated zero gravity	7	Two ambient, five thermal-vacuum; one failure to lock down because of improperly lubricated springs in thermal-vacuum test
Certification	A 167-in. -tread-radius landing gear (10-7-4)	To evaluate functionally	Simulated zero gravity	8	Six ambient; two salt-fog
Certification	A 167-in. -tread-radius landing gear (10-7-4)	To evaluate functionally	Simulated zero gravity; ambient	6	--
Checkout	Apollo 9 to 11	To evaluate functionally (at factory and KSC)	Earth gravity; ambient	37	One failure on Apollo 9 because of jammed insulation and marginal spring tolerances
Flight	Apollo 9 to 11	To deploy operationally	Space	12	--

ASSEMBLY DROP TESTS

A summary of landing-gear drop tests, including single-landing-gear-assembly tests, vehicle structural drop tests, and vehicle tests in a simulated-lunar-gravity environment, is given in table B-II. Almost 90 single-landing-gear-assembly drop tests and approximately 40 vehicle-level tests were performed. All the single-landing-gear-assembly tests and the structural drop tests were performed at the prime contractor facility. The vehicle-level simulated-lunar-gravity tests were conducted at the LRC in support of the landing-gear development program. For these tests, a vehicle with a mass that was representative of the LM and a flight-configuration landing gear were used. Landing-gear-assembly drop tests for single-landing-gear legs were conducted at the prime contractor facility for the three distinct cantilever-type landing-gear designs that reached the hardware-test phase of development (refs. B-11 to B-14). These tests, which were performed under ambient conditions, verified the functional and structural adequacy of the landing-gear assemblies; however, a few tests were conducted with the primary strut in a dry-nitrogen-gas environment to eliminate humidity effects on the strut-bearing dry-film lubricant. The tests were conducted at impact velocities that were representative of the specification vertical touchdown velocities.

TABLE B-II. - LANDING-GEAR DROP-TEST SUMMARY

Type of test	Configuration	Test objectives	Environment	Number of drops
Development	A 160-in. -tread-radius single-landing-gear assembly	To evaluate basic landing-gear functional and structural design concepts	Earth gravity; ambient	27
Development	A 167-in. -tread-radius single-landing-gear assembly	To evaluate functional and structural concepts	Earth gravity; ambient	24
Design verification	A 167-in. -tread-radius (10-7-4) single-landing-gear assembly	To evaluate functional and structural concepts	Earth gravity; ambient	33
Certification ^a	A 167-in. -tread-radius (10-7-4) single-landing-gear assembly	To evaluate the functional, structural, and energy-absorption characteristics following landing-gear exposure to thermal-vacuum and vibration environments	Earth gravity; ambient	4
Certification	LM vehicle structure	To determine the vehicle structural adequacy for critical landing conditions	Earth gravity; ambient	17
Certification	LM vehicle systems	To determine the vehicle systems adequacy for critical landing conditions	Earth gravity; ambient	5
Development ^b	A 167-in. -tread-radius (10-7-4) type (honey-comb cartridges) on mass-simulated LM	To demonstrate landing-gear functional adequacy and two-dimensional toppling stability	Simulated lunar gravity; ambient	21

^aLunar-surface-sensing probe certified in two of these tests.

^bTests conducted at LRC in support of the landing-gear-development program; results correlated with landing-performance analysis.

Although the test facility provided the capability to simulate only vertical touchdown velocities, various types of surfaces could be represented, including rigid surfaces, soils, slopes, and obstructions. The landing gear was attached to a carriage and ballasted to provide the required impact kinetic energy.

The tower drop-test equipment at the prime contractor facility is shown in figure B-2. The landing gear is configured for a symmetrical drop onto a rigid surface. To conserve flight-type footpads, many of the drop tests onto hard surfaces were performed with "workhorse" footpads, which could be used repeatedly. For drop tests into simulated lunar soils, flight-type footpads were used.

Although the test equipment was limited to vertical velocity drops, a wide range of landing-gear impact conditions could be simulated. A landing gear configured for an unsymmetrical drop onto a rigid surface, with the footpad being fully constrained from sliding at impact, is shown in figure B-3. This configuration would result in primary-strut stroking, compression stroking in the upper secondary strut, and tension stroking in the lower secondary strut. A landing gear with a flight-type footpad is shown in figure B-4 after impact into a simulated lunar soil.

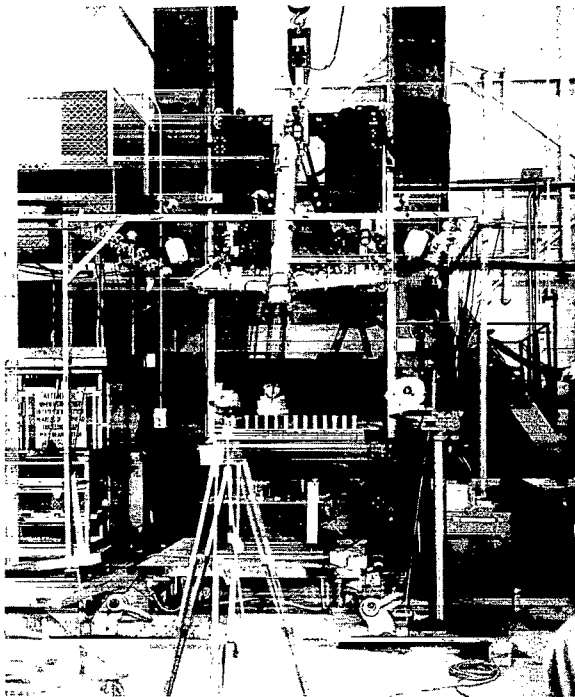


Figure B-2. - Landing-gear drop-test equipment.

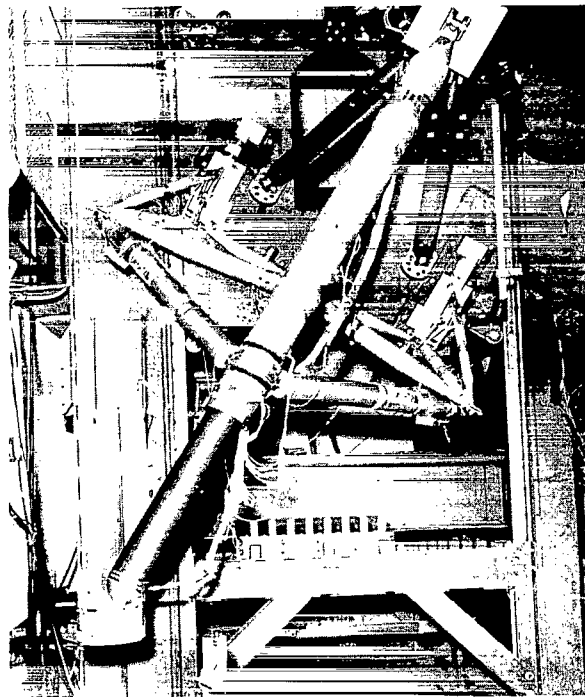


Figure B-3. - Landing gear configured for unsymmetrical drop test.

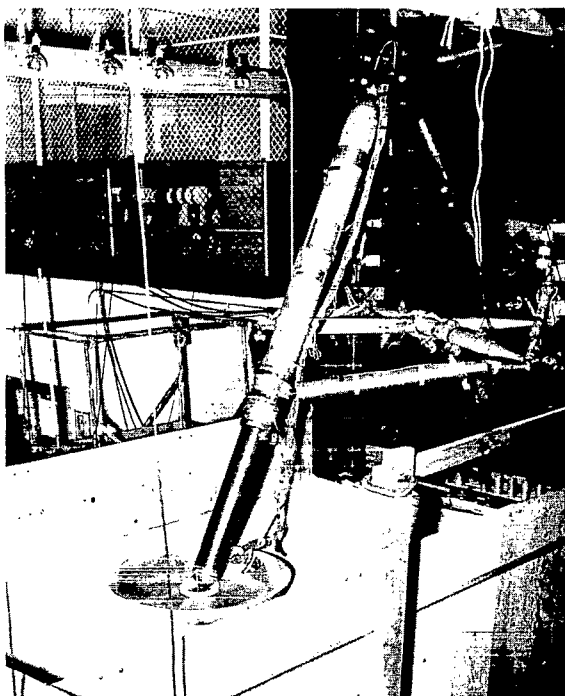


Figure B-4. - Landing gear following drop into simulated lunar soil.

COMPONENT TESTS

Tests at the component level were performed on all major landing-gear components. In addition, extensive component testing was accomplished during development of the primary-strut bearings and the honeycomb energy-absorbing cartridges for both primary and secondary struts.

Bearing Development

It was recognized early in the landing-gear development program that friction in the strut cylinders would have to be maintained within reasonable tolerances to ensure proper control of landing loads induced into the LM structure. Based on this requirement, the prime contractor extensively investigated various types of bearings and bearing lubricants.

Initially, bearing friction tests were performed in early 1965 on a 180-inch-tread-radius landing-gear primary strut (ref. B-15). These tests consisted of an investigation of two types of molydisulfide dry-film lubricant and two bearing shapes. The two bearing shapes considered were cylindrical sleeves and sleeves with slightly convex bearing surfaces. Tests were conducted over a temperature range of $+150^{\circ}$ to -80° F, which resulted in a range of friction coefficients from 0.25 to 0.365.

From February 1965 to March 1966, additional bearing friction tests were performed on a 160-inch-tread-radius landing-gear primary-strut assembly (ref. B-16). Based on the results of these tests, the prime contractor recommended that a molydisulfide dry-film lubricant be used on the primary-strut bearings because it provided a low friction coefficient that remained fairly constant over the temperature range of -80° to $+135^{\circ}$ F and because it had good loading characteristics, a long service life, and good corrosion resistance. For this series of tests, strut side loads ranged from 25 to 100 percent of maximum values, and stroking velocities were as high as 15 ft/sec. Based on the results of these tests, a bearing friction coefficient of 0.20 was generally used in landing-performance and landing-load analyses.

All the previously mentioned testing was conducted under atmospheric conditions. Additional component tests were conducted in a vacuum environment to determine vacuum effects on the dry-film-lubricant friction and wear characteristics. These tests indicate a slight decrease in the friction coefficient in a vacuum. In addition to the tests performed specifically for bearing friction study, the dynamic drop tests of landing-gear assemblies were used to obtain bearing friction-coefficient data and to validate the adequacy of the bearing designs for the primary and secondary struts.

Static Structural Tests

Static structural tests were performed on the landing gear at the major-component level. The components tested were the primary strut, secondary strut, deployment truss, footpad, and lunar-surface-sensing probe. Except for the footpad tests, all the tests were conducted at room temperature, with the results being modified to account for the design structural temperatures.

The primary-strut tests (ref. B-17) were accomplished by applying a static axial load to the strut, with a dynamic side load being applied at the secondary-strut attachment point. These tests verified the dynamic-amplification factors used in the structural analysis and demonstrated the structural adequacy of the strut. Immediately before the flight of Apollo 11, some concern was generated with respect to the landing-gear structural adequacy because of higher predicted temperatures at landing. Using a flight-article primary strut, failure load tests were conducted to determine the landing-gear structural margin (ref. B-18). Static tests of the secondary strut were conducted to demonstrate the functional adequacy of the strut, to demonstrate its structural integrity, to obtain data for correlation with the landing-gear stress-analysis data, and to establish the structural margins of safety (ref. B-19). Unlike the primary strut, which was designed primarily from bending-load data, the secondary strut was designed primarily from axial-load data.

Deployment-truss static tests (ref. B-20) were used to demonstrate the structural integrity of the truss and to provide data for correlation with the structural-analysis

data. All components of the truss were subjected to failure loads. Static ultimate-load tests of the trunnion fitting that attaches the deployment truss to the descent-stage structure also were conducted (ref. B-21).

Footpad-Component Tests

Component tests of various footpad configurations began early in the landing-gear test program. The footpad was required to sustain a 12-lb/in² normal-pressure loading. Because of the unknown characteristics of the landing site, a footpad that could sustain crushing against various obstacles was required. Furthermore, the footpad should plane adequately while sliding over the lunar surface because of a horizontal velocity component at touchdown. This specification was required to preclude the possibility of the footpad digging into the lunar soil and being ripped away from the primary strut.

The footpad component-level tests demonstrated the strength of the footpad when subjected to a uniformly distributed normal load and evaluated the load/stroke characteristics of the footpad when laterally crushed against obstacles of various shapes. Normal-load component tests were conducted at room temperature and at 225° F. The footpad was tested dynamically during the landing-gear-assembly drop tests. Side-load crushing tests were conducted at various load rates and with a variety of obstacle shapes. Lateral crushing of flight-type footpads was also investigated during landing-gear-assembly drop tests onto hard surfaces. Details of the footpad-component tests are contained in references B-22 to B-25.

Honeycomb Energy Absorber

The choice of a method for absorbing the LM impact energy at touchdown is based on several requirements. Because the landing gear is required for only a single landing, the energy absorber does not have to be recycled. The energy absorber must have load/stroke characteristics that are predictable, within close limits, in order to control the loads induced into the vehicle structure. Light weight, compatibility with the space environment, and simplicity are other desirable features. Early in the LM development program, various devices were evaluated in the search for an energy absorber that met these requirements. Initial investigations by the prime contractor indicated that crushable honeycomb could fulfill the requirements and could be developed within the constraints of the Apollo Program schedule.

It became evident early in the honeycomb-development program that several factors influence the load level at which honeycomb crushes. The primary factors are manufacturing tolerances, temperature, and impact velocity. Manufacturing tolerances that have a significant effect on the strength of the honeycomb are the expansion of the hobe (the basic block of alternate layers of aluminum foil and adhesive that is expanded to form the honeycomb core), the foil thickness, the foil material properties, and the adhesive application and curing method. Honeycomb temperature also has a significant effect on the crush strength, with the crush strength decreasing as temperature increases. The crush-load level for an impact velocity is approximately 10 percent greater than the static crush-load level, and this increment is approximately constant over a range of 3 to 12 ft/sec.

These effects were investigated extensively by the prime contractor during development of honeycomb cartridges that were suitable for use on the landing gear. Manufacturing tolerances were reduced to approximately ± 2 percent for the final flight-type cartridges. Velocity effects were accounted for in sizing the cartridges, and temperature effects were reduced to acceptable levels by providing thermal insulation on the landing-gear struts.

The variations in the crush-load levels have been considered in the LM structural-load and landing-performance analyses. In the landing-performance studies, an extensive analysis of the effects of cartridge temperature on vehicle stability and energy-absorption requirements was performed. Honeycomb-development and design-verification-test results are contained in references B-26 to B-30.

LUNAR-SURFACE-SENSING-PROBE QUALIFICATION TESTS

During the course of hardware development, two distinct sensing probes were used in flight. A 4.5-foot probe was used on the Apollo 9 and 10 missions, and a 5.6-foot probe was used on the Apollo 11 mission. Both probe designs underwent complete qualification-test programs. Details of the qualification of the 5.6-foot probe are contained in reference B-31. With the exception of probe certification in drop tests, certification was accomplished by the probe-hardware vendor.

Two probe assemblies were subjected to all significant mission-level environments, including shock, vibration, and thermal-vacuum environments. The electro-mechanical sensing-switch operation was monitored during testing, and the probe-deployment mechanism was checked. Before qualification of the early model 4.5-foot probe, extensive development testing was performed by the vendor under the cognizance of the prime contractor.

CERTIFICATION SUMMARY

All certification-level tests are listed in table B-III. Also provided is a brief description of the tests, information about the level of assembly, and whether the test was an original requirement or was added because of a design change or a new qualification requirement. The flight hardware is compared with the certified hardware in table B-IV. Some design changes did not necessitate complete hardware recertification for various reasons. These design changes, together with the reasons the flight configuration was considered to be adequate, are also listed in table B-IV. Where practical, analysis was performed to demonstrate the adequacy of the flight hardware; however, in some cases, configuration differences were so minor that the flight hardware was determined to be adequate by design similarity.

TABLE B-III. - CERTIFICATION SUMMARY OF THE LM LANDING-GEAR SUBSYSTEM

Title of test	Type of test	Effectivity	Requirement
Qualification test of 4.5-ft lunar-surface-sensing probe	Component	Apollo 9 and subsequent	Original
Landing-gear deployment in a thermal-vacuum environment	Landing-gear assembly	Apollo 9 and subsequent	Original
Landing-gear deployment in a salt-fog environment	Landing-gear assembly	Apollo 9 and subsequent	Original
Landing-gear and landing-gear-uplock compatibility	Landing-gear assembly	Apollo 9 and subsequent	Original
Footpad structural adequacy	Analysis	Apollo 11 and subsequent	Original
Lunar-surface-sensing-probe drop tests	Landing-gear assembly	Apollo 11 and subsequent	Original
Landing-gear-assembly drop tests	Landing-gear assembly	Apollo 11 and subsequent	Original
Delta-qualification test of 4.5-ft lunar-surface-sensing probe	Component	Apollo 11 and subsequent	Delta-qualification for new vibration-acceptance-test requirement
Compatibility of 5.6-ft lunar-surface-sensing probe with landing-gear uplock	Landing-gear assembly	Apollo 11 and subsequent	Delta-qualification requirement because of lengthened probe
Qualification test of 5.6-ft lunar-surface-sensing probe	Component	Apollo 11 and subsequent	Requalification because of new probe length
Landing-performance adequacy of LM	Analysis	Apollo 11 to 14	Original
Landing-gear response to launch and boost vibration	Vehicle	Apollo 9 and subsequent	Original
Landing-gear response to descent-engine vibration	Vehicle	Apollo 9 and subsequent	Original
Structural drop test of LM	Vehicle	Apollo 11 to 14	Original

TABLE B-IV. - COMPARISON OF CERTIFIED AND FLIGHT-CONFIGURATION HARDWARE

Hardware	Qualification configuration	Flight configuration	Rationale
Significant differences			
Thermal blankets and plume shielding	None	Flight blankets and shielding	Thermal analysis and functional tests
Landing-gear-deployment spring	Nine-leaf spring in thermal-vacuum test	10-leaf spring	Delta-qualification with 10-leaf spring and thermal blankets installed
Honeycomb cartridges	No node bond strength requirement	Node peel strength acceptance-test requirement	Quality control requirement
Strut-bearing clearances	No requirement for high temperatures caused by fire until touchdown heating	Clearances increased to allow for thermal expansion	Thermal analysis and functional tests
Minor differences			
Sonic inspection of machine parts	None	Parts received sonic inspection	Quality-control requirement
Liquid shim	None	Liquid shim on mating surfaces	Stress-corrosion prevention
Suit hazards	Cotter pins and nuts with sharp edges	Cotter pins removed and sharp-edged nuts capped	Crew systems requirement
Backup visual downlock indicator for landing gear	None	Visual indicator consisting of paint stripes on downlock	Crew systems requirement
Footpad restraint straps	Aluminum alloy	Titanium	Analysis
Overcenter strap	Strap on landing gear for vibration tests	No overcenter strap	Analysis
Uplock retaining nut and bolt	Standard bolt and self-locking nut	Shoulder bolt and castelated nut	Analysis
Lunar-surface-sensing probe	The 4.5-ft probe in thermal-vacuum deployment and in drop tests	The 5.6-ft probe	Ambient deployment test and analysis

REFERENCES

- B-1. Anon.: Test Results for Landing Gear Assembly Tests, Section B — Results of the 160" Landing Gear Deployment Tests. Rept. LTR 904-14001B, Grumman Aircraft Engineering Corp., Jan. 21, 1966.
- B-2. Anon.: Test Results for the Landing Gear Assembly Tests, Section C — Results of the 160" Landing Gear Deployment Tests After Salt Fog. Rept. LTR 904-14001C, Grumman Aircraft Engineering Corp., May 25, 1966.
- B-3. Anon.: Results of the 167" Semi-Tread (10-7-4) Landing Gear Vertical Deployment Tests. Rept. LTR 904-14005, Grumman Aircraft Engineering Corp., Feb. 2, 1967.
- B-4. Anon.: Results of Thermal Vacuum Test of 167" Semi-Tread (10-7-4) Landing Gear Assembly. Rept. LTR 904-14012, Grumman Aircraft Engineering Corp., Mar. 13, 1967.
- B-5. Anon.: Results of the Deployment Tests (Horizontal) of the 167" Semi-Tread (10-7-4) Landing Gear Assembly. Rept. LTR 904-14020, Grumman Aircraft Engineering Corp., Apr. 6, 1967.
- B-6. Anon.: Results of 167" (10-7-4) Landing Gear Vertical Deployment Tests Using Full Insulation. Rept. LTC 904-14024, Grumman Aircraft Engineering Corp., Sept. 18, 1967.
- B-7. Anon.: Results of Landing Gear Deployment Tests (With Revised Insulation Configuration). Rept. LTR 904-14036, Grumman Aircraft Engineering Corp., June 20, 1969.
- B-8. Anon.: Results of the 167" (10-7-4) Landing Gear Deployment Tests With the Revised Thermal Insulation. Rept. LTC 904-15008, Grumman Aircraft Engineering Corp., Aug. 8, 1969.
- B-9. Anon.: Test Results of the Certification Test of the LM Landing Gear Deployment System Equipped With Environmental Protective Covers. Rept. LTR 904-14014, Grumman Aircraft Engineering Corp., Feb. 27, 1967.
- B-10. Anon.: Test Results of the LM Landing Gear Component Development Test. Results of the Component Tests of the LM Landing Gear Deployment Spring LSC320-202. Rept. LTC 904-14016, Grumman Aircraft Engineering Corp., Feb. 15, 1967.
- B-11. Anon.: Test Results for Landing Gear Assembly Tests, Section A — Test Results for 160" Semi-Tread Landing Gear Assembly Tests. Rept. LTR 904-14001B, Grumman Aircraft Engineering Corp., Sept. 15, 1966.

- B-12. Anon.: Test Results for Landing Gear Assembly Tests, Section E — Test Results for 167" Semi-Tread Landing Gear Assembly Tests. Rept. LTR 904-14001D, Grumman Aircraft Engineering Corp., June 9, 1967.
- B-13. Anon.: Results of the LM 167 Inch Semi-Tread (10-7-4) Landing Gear Assembly Drop Test Program. Rept. LTR 904-14009, Grumman Aircraft Engineering Corp., Oct. 12, 1967.
- B-14. Anon.: Results of Drop Tests for Certification of LM 167 Inch Semi-Tread (10-7-4) Landing Gear Assembly. Rept. LTR 904-14013, Grumman Aircraft Engineering Corp., Aug. 25, 1967.
- B-15. Anon.: Test Report for the Development of Linear Bearing Friction Materials 180" Strut. Rept. LTR 320-5, Grumman Aircraft Engineering Corp., Mar. 16, 1966.
- B-16. Anon.: Test Report for the Cantilever Primary Strut Assembly Friction Load Test 160" Strut. Rept. LTR 320-6, Grumman Aircraft Engineering Corp., Apr. 15, 1966.
- B-17. Anon.: Results of the Structural Tests of the 167" (10-7-4) Landing Gear Primary Strut. Rept. LTR 904-14003, Grumman Aircraft Engineering Corp., Sept. 18, 1967.
- B-18. Anon.: Results of the Primary Strut Failing Load Test. Rept. LTR 904-14035, Grumman Aircraft Engineering Corp., June 18, 1969.
- B-19. Anon.: Results of Functional and Structural Tests of LDW 320-23553 Secondary Strut Assembly and (10-7-4) Ball Joint Assembly. Rept. LTR 904-14004, Grumman Aircraft Engineering Corp., Sept. 30, 1967.
- B-20. Anon.: Results of Structural Tests of the 167" (10-7-4) Landing Gear Deployment Truss. Rept. LTR 904-14007, Grumman Aircraft Engineering Corp., July 19, 1967.
- B-21. Anon.: Report of Landing Gear Trunnion Failing Load Investigation. Rept. LTR 904-14034, Grumman Aircraft Engineering Corp., June 17, 1969.
- B-22. Anon.: Results of the LEM Landing Gear Component Development Tests, Section D — Results of the Static Test of the LEM Landing Gear Footpad LSK-320-10702. Rept. LTR 904-10001D, Grumman Aircraft Engineering Corp., Feb. 14, 1966.
- B-23. Anon.: Results of the LEM Landing Gear Component Development Tests, Section J — Results of the Static Test of the LEM Landing Gear Footpad LSK-320-10704. Rept. LTR 904-10001. Grumman Aircraft Engineering Corp., Feb. 28, 1966.

- B-24. Anon.: Results of the LEM Landing Gear Component Development Tests, Section M — Results of the Static Test of the LEM Landing Gear Footpad LSK-320-10707. Rept. LTR 904-10001, Grumman Aircraft Engineering Corp., Feb. 12, 1966.
- B-25. Anon.: Results of the LEM Landing Gear Component Development Tests, Section Q — Results of the Normal Load Test of Footpad LTM-320-H-10701. Rept. LTR 904-10001, Grumman Aircraft Engineering Corp., Aug. 9, 1966.
- B-26. Anon.: Design Data Derived From Preliminary Testing of Honeycomb Cartridge. Rept. LTR 320-4, Grumman Aircraft Engineering Corp., Jan. 14, 1966.
- B-27. Anon.: Results of the LEM Landing Gear Component Development Tests, Section B — Crushable Cartridges — Intermediate and Full Size. Rept. LTR 904-10001, Grumman Aircraft Engineering Corp., Jan. 6, 1967.
- B-28. Anon.: Results of the LEM Landing Gear Component Development Tests, Section P — Crushable Honeycomb Cartridges for the 160" and 167" Landing Gear Assemblies. Rept. LTR 904-10001, Grumman Aircraft Engineering Corp., Apr. 5, 1967.
- B-29. Anon.: Results of Tests on the 167" (10-7-4) Landing Gear Honeycomb Cartridges — Block I. Rept. LTR 904-14010, Grumman Aircraft Engineering Corp., June 16, 1967.
- B-30. Anon.: Design Data Derived From the Intermediate Testing of Honeycomb Cartridges. Rept. LTR 320-13, Grumman Aircraft Engineering Corp., Aug. 18, 1967.
- B-31. Anon.: Final Report — Qualification Test of the 5.6 Foot Lunar Surface Sensing Probe for LM. Rept. 8342, rev. A, Edo Corp., Mar. 1969.

APPENDIX C

DETAILED CONFIGURATION DESCRIPTION

PRIMARY STRUT

A sketch of the primary strut is shown in figure 6. The strut consists of a lower inner cylinder that fits into an upper outer cylinder to provide compression stroking at touchdown. The primary strut (which includes an outer-cylinder upper universal fitting attached to the LM-descent-stage outrigger assembly and an inner-cylinder lower ball fitting attached to the footpad) is approximately 10 feet in length in the un-stroked position. Within the inner cylinder is the energy-absorbing material, a crushable aluminum-honeycomb core that has design load/stroke characteristics as shown in figure 7. The honeycomb characteristics and design features are discussed in more detail in appendix B.

The primary-strut structural safety factor is 1.35, and the safety factor on all fittings is 1.50. The strut is manufactured from type 7178 aluminum alloy. The inner cylinder is nominally 5.5 inches in diameter. The wall thickness ranges from 0.150 inch near the ball fitting, where design bending moments are relatively small, to approximately 0.255 inch near the outer-cylinder juncture, where the design bending moment is more than 300 000 in-lb.

To control the axial loads imposed on the primary strut because of stroking, the honeycomb crush loads and the axial load that results from friction in the bearings must be controlled within specified limits. The development of the primary-strut bearings required a significant effort and is discussed in detail in appendix B. The cantilever-type design of the landing gear results in high lateral loads on the primary strut because of secondary-strut axial loads, which must be considered in the bearing design. The aluminum-sleeve-type bearing over which the cylinder slides is coated with a molydisulfide dry-film lubricant. For the upper bearing, the inner surface of the outer cylinder acts as the sleeve, and the inner-cylinder bearing surface is a machined part of the cylinder. All bearing surfaces are coated with the molydisulfide dry-film lubricant. The lower bearing is threaded into the lower end of the outer cylinder. The outer surface of the inner cylinder, which is also coated with the dry-film lubricant, slides against the bearing surface. The strut is capable of a 32-inch stroke, which results in a nominal energy-absorption capability of 254 000 in-lb per primary strut.

The distance between the upper and lower bearings is approximately 33 inches before stroking. Based on a bearing diameter of 5.5 inches, the bearing overlap ratio is 6.0, with the ratio increasing as the landing gear strokes. In the design of a stroking member where binding is intolerable and where loads caused by bearing friction must be controlled, the ratio should be at least 3.0. However, the ratio must be larger if the members are subjected to large side loads, as is the case with the primary strut.

SECONDARY STRUT

The secondary strut (fig. 8) is similar to the primary-strut basic design in that it consists of an inner cylinder that slides into an outer cylinder during stroking. The honeycomb shock and energy-absorbing material is contained within both the inner and outer cylinders and has nominal load/stroke characteristics (fig. 9).

The secondary strut is approximately 4 feet in length when unstroked, and the outer cylinder is approximately 4.5 inches in diameter. The outer-cylinder ball fitting is attached to a socket on the primary strut, and the inner-cylinder end fitting is attached to the deployment truss. The strut cylinders are manufactured from type 2024 aluminum. The wall thickness varies from 0.027 inch for the outer cylinder to 0.033 inch for the inner cylinder.

Because the secondary strut is designed primarily to sustain axial loads (with only small lateral loads), the problem of designing bearings for stroking was relatively simple. The design lateral-inertial load factor for the strut is 20g. The main secondary-strut bearing consists of a Teflon-impregnated fabric sleeve that is bonded to the inner wall of the outer cylinder at the open end of the cylinder (fig. 8). The sleeve is approximately 3.25 inches long and approximately 0.014 inch thick. A similar type of bearing is attached to the inner cylinder.

As shown in figure 9, the secondary strut is capable of absorbing energy for both tension and compression stroking. The nominal energy-absorption capability is 62 000 in-lb in tension and 54 000 in-lb in compression, for a total of 116 000 in-lb per secondary-strut assembly.

Once a secondary strut is stroked, for either tension or compression, the slack that results from the stroke must be taken up before energy absorption can occur in the opposite direction. This no-load slack condition is unlikely to occur in an actual landing situation and presented no problems during landing-gear-assembly ground tests.

DEPLOYMENT TRUSS

The deployment-truss assembly (fig. 4) consists of two main crossmembers and four side members. In the deployed position, the truss acts as a rigid structure to which the secondary struts are attached. The landing-gear deployment and downlock mechanism is attached to the deployment truss and pulls on the truss lower side members to deploy the entire landing-gear assembly. The upper side members of the truss lock into the downlock mechanism, which is attached to the descent-stage structure. In the stowed position, both the truss and the entire landing gear are kept rigid by two uplock chocks (fig. 2), which extend downward from the descent stage. In the stowed position, each chock has approximately 350 pounds of compression load, and the uplock strap (fig. C-1) has approximately 1100 pounds of tension load. These loads prevent landing-gear movement that might result from launch and boost vibration. The major components of the deployment truss are fabricated from type 7079 and type 7178 aluminum alloy.

DEPLOYMENT AND DOWNLOCK MECHANISM

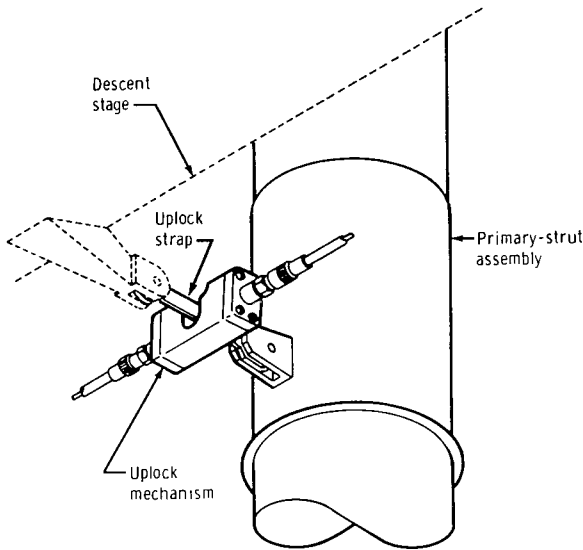
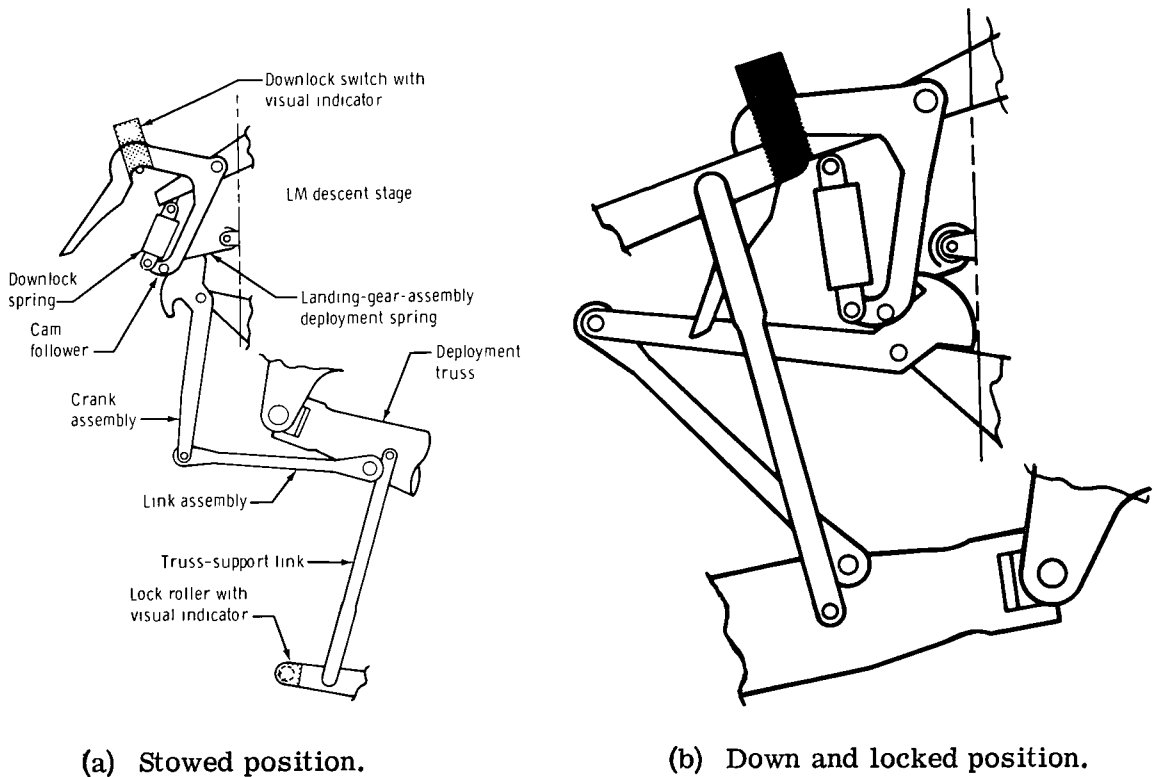


Figure C-1. - Landing-gear uplock mechanism.

The deployment and downlock mechanism (fig. C-2) performs two distinct operations: deployment of the landing-gear assembly by a linkage attached to the deployment truss and rigid latching of the landing gear in place after deployment has been accomplished.

The deployment portion of the mechanism consists of a spring and a mechanical linkage. The spring consists of 10 individual stainless steel leaves. The leaves, which are coated with the dry-film lubricant, slide freely over one another as the spring rolls up. The



(a) Stowed position.

(b) Down and locked position.

Figure C-2. - Landing-gear deployment and downlock mechanism.

linkage is attached from the descent-stage structure to the lower side member of the landing-gear deployment truss. One end of the deployment spring is attached to this linkage; the other end is coiled around a roller that is attached to the descent-stage structure. In the stowed position, energy is stored in the deployment springs. When the uplock strap is severed to release the landing gear, the deployment spring rolls up and pulls on the linkage, causing the deployment truss to rotate and deploy the landing gear.

The downlock portion of the mechanism consists of a spring-loaded latch attached to the descent-stage structure and a latch roller on the upper side member of the deployment truss. When the landing gear is retracted, the latch is held open because the cam follower rests on the cam of the cam idler crank. As the landing gear deploys, the cam rotates; and, at full deployment, the cam follower drops off the cam ramp, which allows the spring to snap the latch over the latch roller. This secures the roller against a stop on the structure. As latching occurs, two electrical downlock switches are actuated, which closes the circuit to the landing-gear-deployment indicator in the cabin. Both downlocks on each landing-gear assembly must be properly latched for the landing-gear-deployment indicator to signal that the landing gear is down and locked.

In the event of a malfunction of the landing-gear-deployment electrical circuitry, a visual backup indicator has been devised to allow the command module pilot to verify that all downlocks have latched. The visual indicator consists of a red luminescent stripe painted on both sides of the downlock latch and on the end of the latch roller that is attached to the truss-roller support member (fig. C-2). If the landing gear is properly locked, the stripe shows as an unbroken straight line. If a downlock is not achieved, the paint stripe shows as a broken line.

LUNAR-SURFACE-SENSING PROBE

Attached to each footpad except the one on the forward landing gear is a 5.6-foot-long lunar-surface-sensing probe that is designed to sense lunar-surface proximity and signal the pilot to cut off the descent engine. The lunar-surface-sensing probe is shown in the stowed and deployed positions in figure 2. The probe consists of two major components: the boom assembly, which contains a deployment mechanism, and the probe-switch subassembly, which is an electromechanical device. Actuation of the switch on contact with the lunar surface causes two blue lunar-contact lights to be illuminated in the cabin, which signals the crew to shut down the descent engine manually.

The probe boom assembly consists of two components that are hinged at the deployment mechanism. The probe boom is made from type 2024 aluminum tubing and is approximately 1.25 inches in diameter. The upper portion of the boom is bolted to the footpad. The probe-deployment mechanism (fig. C-3) consists of two fittings connected by a pin joint.

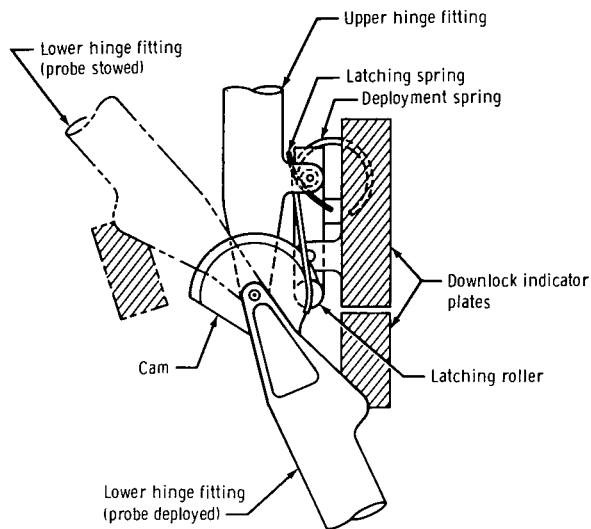


Figure C-3. - Lunar-surface-sensing-probe-deployment mechanism.

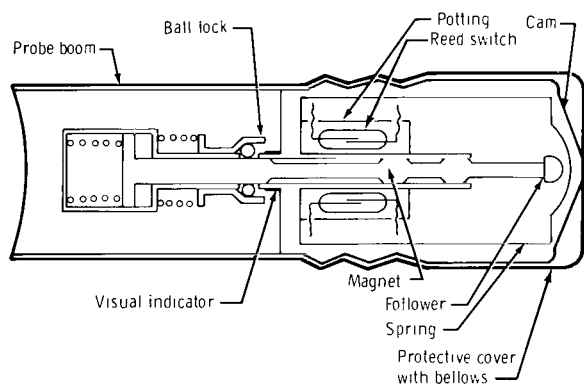


Figure C-4. - Lunar-surface-sensing-probe switch.

When the switch is actuated, it latches in the open position, causing the lunar-contact light to remain illuminated even after failure of the boom structure beneath the descending footpad.

FOOTPAD

The dish-shaped footpad, which was designed for a 1.0-lb/in^2 static-bearing-strength surface, is 37 inches in diameter and approximately 7 inches deep. The footpad is attached to the primary strut by a ball-and-socket joint (fig. C-5). Before touchdown on the lunar surface, the footpad is restrained from moving by four restraint straps attached between the footpad hub and the primary-strut end fitting. At touchdown, these

Attached to the lower hinge fitting and to the locking link are downlock indicator plates that are painted a luminous green. When the probe is properly locked down, the plates form an unbroken straight line; otherwise, they show as a broken line. These visual indicators are the only positive means of determining that the probes are properly locked.

The second major component of the probe is the sensing-switch subassembly. A diagram of the switch, including the mechanism that allows switch actuation from vertical, horizontal, or combined loads, is shown in figure C-4. This mechanism, which is housed within a container, allows switch actuation on a surface with a bearing strength as low as 3 lb/in^2 . Loading the mechanism moves a cam that actuates a plunger in the center of the switch. As the plunger actuates, it moves a magnet that allows the contacts on two reed switches within the switch to open. When the switches open, the two lunar-contact lamps in the cabin are illuminated. The circuitry is redundant in that both of the reed switches within a single probe must open to produce a lunar-contact signal. This provides for the possibility of a switch failed in the open position. Further reliability is provided by the three probes, any one of which can activate the lunar-contact circuitry. Therefore, if a switch fails closed in one probe, the second probe to contact the surface will cause a lunar-contact signal.

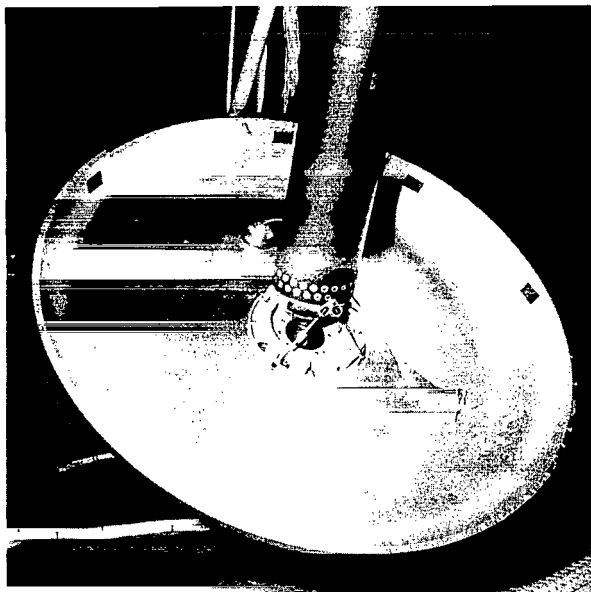


Figure C-5. - Landing-gear footpad.

straps break, allowing the footpad to rotate as necessary during sliding. The straps are designed to fail when a moment of 3340 in-lb is applied to rotate the pad. The footpad, constructed of aluminum honeycomb bonded to machined aluminum face sheets, has been designed to withstand considerable damage from impacting rocks, craters, ledges, and so forth. The results of ground tests to determine the ability of the footpad to remain functional even after considerable impact damage are discussed in the section of appendix B entitled "Footpad-Component Tests."

The type 7075 machined-aluminum face-sheet thickness ranges from a nominal 0.0085 to 0.0165 inch on the lower surface and from 0.0085 to 0.050 inch on the upper surface. The footpad core is constructed of type 2024 and type 5052 honeycomb.

PREFLIGHT CHECKOUT

To ensure proper operation of the landing gear during flight, extensive ground checkout of the hardware is conducted at the factory and at the launch site (fig. C-6). Factory checkout ensures that the landing gear is operating properly and that any operating deficiencies can be corrected before shipment. Checkout at the NASA John F. Kennedy Space Center provides a final check before installation of the LM and the LM adapter.

Checkout requirements at the prime contractor facility and at the launch site are similar and consist of mechanical and electrical checks. All landing-gear checkout is performed in an ambient environment that meets spacecraft cleanliness requirements. Electrical checks consist of testing the landing-gear downlock-switch and probe-switch circuitry. End-to-end circuitry tests are made between the switches and the cabin indicators. Mechanical checks are made of the landing-gear probe-deployment and downlock mechanism, the probe release mechanism, the landing-gear downlock switches, and the lunar-surface-sensing-probe switches.

The lunar-surface-sensing-probe switches are subject to inadvertent activation and latching during vehicle checkout at the launch site. For this reason, a final visual check of these switches is performed approximately 18 hours before launch, just before closeout of the SLA. This is the final vehicle check performed before the work platforms are removed from around the LM. Functional checks of the struts are not practical after installation of the honeycomb cartridges; however, such checks are performed during landing-gear assembly.

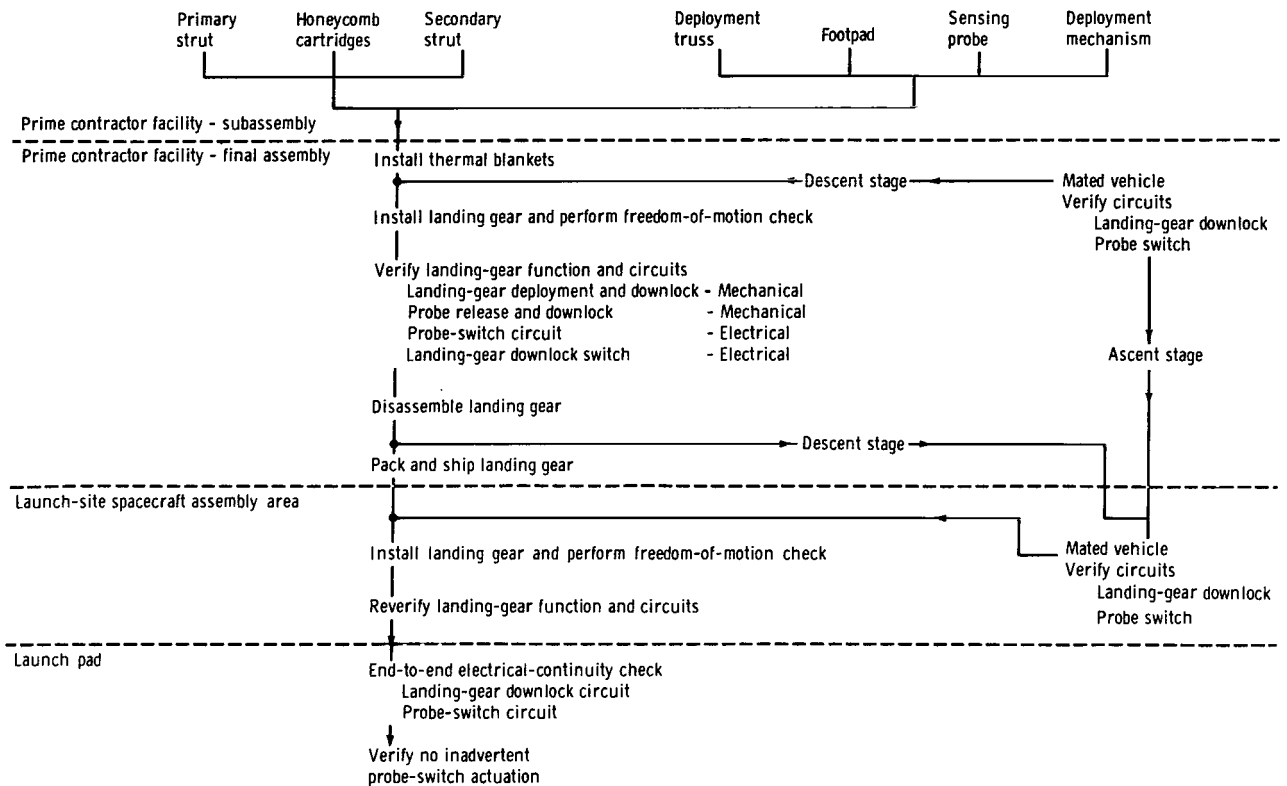


Figure C-6. - Landing-gear-assembly test flow.

Because the landing gear is exercised considerably before the flight and because much work is performed in the vicinity of the landing gear during vehicle checkout, certain basic hazards have been identified with regard to the hardware. The item of greatest concern has been the possibility of misuse of landing-gear hardware inside the SLA where the working area is cramped. Several instances of inadvertent actuation of probe switches have occurred on vehicles being readied for launch. In addition, concern for misuse of landing-gear hardware, such as using struts for handholds or footholds, prompted a special training program for personnel working inside the SLA to preclude any further incidents.

NATIONAL AERONAUTICS AND SPACE ADMINISTRATION
WASHINGTON, D.C. 20546

OFFICIAL BUSINESS
PENALTY FOR PRIVATE USE \$300

FIRST CLASS MAIL

POSTAGE AND FEES PAID
NATIONAL AERONAUTICS AND
SPACE ADMINISTRATION



NASA 451

023 001 01 0 31 721526 500903DS
DEPT OF THE AIR FORCE
AF WEAPONS LAB (AFSC)
TECH LIBRARY/WBOL/
ATTN: W L O J BOWMAN, CHIEF
KIRTLAND AFB NH 03717

POSTMASTER: If Undeliverable (Section 158
Postal Manual) Do Not Return

"The aeronautical and space activities of the United States shall be conducted so as to contribute . . . to the expansion of human knowledge of phenomena in the atmosphere and space. The Administration shall provide for the widest practicable and appropriate dissemination of information concerning its activities and the results thereof."

— NATIONAL AERONAUTICS AND SPACE ACT OF 1958

NASA SCIENTIFIC AND TECHNICAL PUBLICATIONS

TECHNICAL REPORTS: Scientific and technical information considered important, complete, and a lasting contribution to existing knowledge.

TECHNICAL NOTES: Information less broad in scope but nevertheless of importance as a contribution to existing knowledge.

TECHNICAL MEMORANDUMS: Information receiving limited distribution because of preliminary data, security classification, or other reasons.

CONTRACTOR REPORTS: Scientific and technical information generated under a NASA contract or grant and considered an important contribution to existing knowledge.

TECHNICAL TRANSLATIONS: Information published in a foreign language considered to merit NASA distribution in English.

SPECIAL PUBLICATIONS: Information derived from or of value to NASA activities. Publications include conference proceedings, monographs, data compilations, handbooks, sourcebooks, and special bibliographies.

TECHNOLOGY UTILIZATION PUBLICATIONS: Information on technology used by NASA that may be of particular interest in commercial and other non-aerospace applications. Publications include Tech Briefs, Technology Utilization Reports and Technology Surveys.

Details on the availability of these publications may be obtained from:

SCIENTIFIC AND TECHNICAL INFORMATION OFFICE

NATIONAL AERONAUTICS AND SPACE ADMINISTRATION

Washington, D.C. 20546